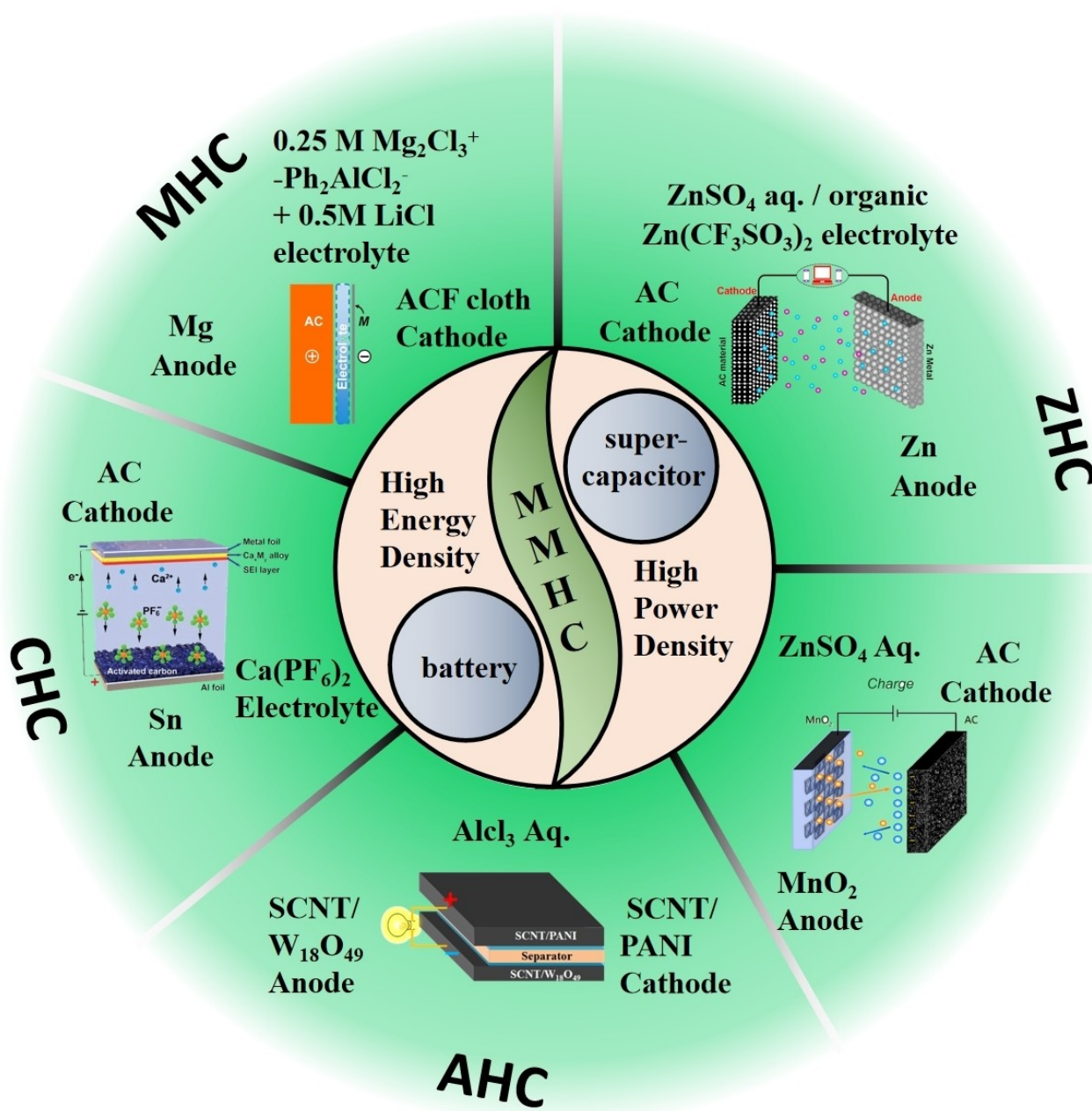


VIP Very Important Paper

Special
Collection

Recent Progress and Challenges in Multivalent Metal-Ion Hybrid Capacitors

Xueang Yu^{+[a]}, Xuhao Wu^{+[a]}, Yuxuan Liang^{+[a]}, Kaijie Liang,^[a] Shuoji Huang,^[a] Kunjian Li,^[a] Mingjian Chen,^[a] Shaofeng Liu,^[a] Na Li,^{*[a]} and Zhicong Shi^{*[a]}



Multivalent metal-ion hybrid capacitors (MMHCs) have drawn much attention in recent years because of their advantages of high energy density (similar to metal-ion batteries) as well as high power density, high rate capability, and ultra-long cycle life. However, there are still challenges in developing high-performance MMHCs, e.g., high-capacity capacitive materials are particularly needed to be developed to match high-energy battery-type electrodes. Therefore, designing novel electrode materials and exploring suitable electrolytes are of particular

importance. Herein, we focus on the recent progress of MMHCs in relation to their cathode/anode materials, electrolytes, electrochemical properties, and energy storage mechanisms. Additionally, the current challenges or bottlenecks and future research trends regarding MMHCs are summarized. This review provides a comprehensive understanding of the research framework of MMHCs and will be beneficial in the development of high-performance MMHC devices.

1. Introduction

As the main force of new energy storage systems, secondary batteries are being commonly used in various electronic devices owing to their high energy density.^[1] However, the low rate performance (low power density),^[2] insufficient resources^[3] (such as lithium), and lack of safety highly limit their practical application.^[4] In contrast, supercapacitors are types of capacitors, and they possess rapid charge-discharge capability (high-power density), ultra-long cycle life, and excellent cycling stability; however, they have relatively low energy density.^[5] Concurrently, researchers have successfully integrated the advantages of both battery- and capacitor-type devices in one energy storage system known as a metal ion hybrid capacitor (MIHC).^[6] In a typical MIHC device, battery- and capacitor-type materials are utilized as Faradaic and capacitive counter electrodes, respectively.

Among MIHC devices, alkali metal ion (Li^+ , Na^+ , and K^+) hybrid capacitors have been extensively studied.^[7] Nevertheless, the high reactivity of alkali metals can cause safety problems in their corresponding energy storage systems. Moreover, the accelerating commercial applications of secondary batteries (e.g., lithium ion batteries) in various fields are expected to increase the cost of the scarce lithium resources for lithium ion hybrid capacitors.^[8] Thus, novel energy storage hybrid capacitors were developed based on multivalent metal ions (Ca^{2+} , Mg^{2+} , Al^{3+} , and Zn^{2+}) called as multivalent metal ion hybrid capacitors (MMHCs),^[6c,9] and new multivalent ion storage mechanisms were proposed.^{[9c,10][11]} MMHCs exhibit many interesting characteristics: i. abundant resources, ii. stability and high safety, iii. rapid charge-discharge kinetics owing to the low binding energy (for specific materials^[11]), and iv. high energy density, which is ascribed to the multi-electronic energy storage process.^[12] However, the key to fully demonstrating the advantages of

multivalent ions and realizing MMHC devices having both high power density and high energy density is to develop suitable cathode/anode materials and electrolytes to match the different multivalent ions.

Herein, the recent progress and challenges of MMHC devices, including battery-type electrode materials, capacitor-type electrodes, and electrolytes, were reviewed. First, the device assembly modes and energy storage mechanisms of MMHCs, batteries, and supercapacitors were compared and analyzed in detail. Subsequently, we focused on four types of MMHC devices (Figure 1): calcium-ion hybrid capacitors (CHCs), magnesium-ion hybrid capacitors (MHCs), zinc-ion hybrid capacitors (ZHCs), and aluminum-ion hybrid capacitors (AHCs). The electrode materials and electrolytes employed in each device were summarized, and some related multivalent ion batteries were discussed to provide more alternatives for the development of high-performance MMHC electrodes.

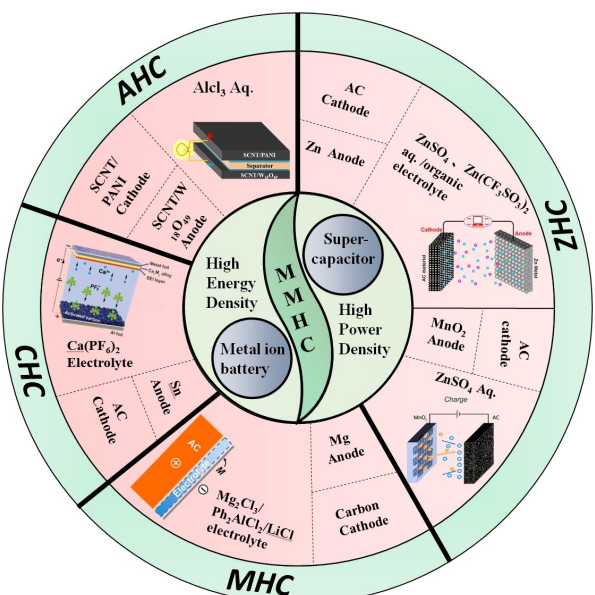


Figure 1. Illustration of four kinds of multivalent ion hybrid capacitors reported previous. The insets are electrode materials/electrolyte and device construction corresponding to ZHC, MHC, CHC and AHC devices. Reproduced from Refs. [9c, 10] with permission: Copyright (2018) Elsevier; [10a] Copyright (2017) Elsevier; [9c] Copyright (2019) Elsevier; [10c] Copyright (2019) Wiley-VCH; [10e] Copyright (2016) American Chemical Society; [10d] Copyright (2017) American Chemical Society. [10b]

[a] X. Yu,[†] X. Wu,[†] Y. Liang,[†] K. Liang, S. Huang, K. Li, M. Chen, S. Liu, N. Li, Prof. Z. Shi
School of Materials and Energy
Guangdong University of Technology
Guangzhou, 510006, China
E-mail: lina150907@gdut.edu.cn
zhicong@gdut.edu.cn

[†] These authors contributed equally to this work.

Special Collection An invited contribution to a Special Collection dedicated to Metal-Ion Hybrid Supercapacitors

Furthermore, the current challenges and future developments of MMHCs were prospected. This review will provide a comprehensive understanding of MMHC capacitors, which will

benefit the future design and assembly of high-energy-density MMHC devices.



Xue'ang Yu is currently a junior student majored in microelectronic science and engineering, in the school of material and energy, Guangdong University of Technology. He joined the Dr. Li's research team in 2018. He is mainly interested in nano energy materials and devices, such as metal ion batteries and supercapacitors.



Xuhao Wu is now pursuing his master degree under direction of associate Prof. Na Li in the School of materials and energy, Guangdong University of Technology. He is mainly interested in the synthesis of nanomaterials and their energy applications.



Yuxuan Liang is a junior in the School of materials and energy, Guangdong University of technology, majoring in microelectronics science and engineering. He followed Associate Professor Li Na to focus on metal ion energy storage equipment.



Kaijie Liang is a junior student major in microelectronics science and engineering, School of materials and energy, Guangdong University of Technology. He joined the Dr. Li's research team in 2018. He is interested in developing multivalent metal ions energy storage equipment.



Shuoji Huang is currently a junior student in the school of materials and energy, Guangdong University of Technology. He joined the Dr. Li's research team in 2019. His main direction of research addresses flexible new energy materials and devices.



Kunjian Li is a junior student major in microelectronics science and engineering, School of materials and energy, Guangdong University of Technology. He joined the Dr. Li's research team in 2019. He is mainly interested in multivalent metal batteries and capacitors.



Mingjian Chen is now a B. Eng. from school of material and energy, Guangdong University of Technology. He is studying microelectronics science and engineering. He joined the Dr. Li's research team in 2019. He is mainly interested in metal ion batteries and flexible supercapacitors.



Shaofeng Liu is now pursuing his master degree under direction of Prof. Na Li in the school of materials and energy, Guangdong University of Technology. He is mainly interested in the synthesis of nanomaterials and their applications in zinc ion battery.



Na Li is currently an Associate Professor in the school of materials and energy, Guangdong University of Technology. She received her Ph.D. degree from Sun Yat-sen University in 2015. She obtained Science and Technology Innovation Youth Top Talent of "Guangdong Special Support Program". Dr. Li's interest lies in developing nano energy materials and devices.



Zhicong Shi received his Ph.D. in physical chemistry from Xiamen University in 2005. He joined Dalian University of Technology as an Associate Professor after a postdoctoral research fellowship in University of Alberta, Canada. Now he is a Professor in the School of Materials and Energy, Guangdong University of Technology. His current research interests focus on design, characterization, and understanding the working mechanism of materials for supercapacitors, batteries and fuel cells.

2. Research Progress and Challenges of MMHCs

2.1. Energy Storage Mechanism of MMHCs

A metal ion battery is a type of rocking chair battery, in which metal cations flow back and forth between the cathode and anode materials.^[13] Consider a lithium ion battery ($\text{LiCoO}_2/\text{graphite}$) as an example.^[14] As shown in Figure 2a, during the charging process, an external voltage is applied to the battery, and the cathode starts releasing lithium ions, expressed as follows: $\text{LiCoO}_2 - xe^- \rightarrow \text{Li}_{1-x}\text{CoO}_2 + x\text{Li}^+$. The lithium ions migrate to the anode through the electrolyte and embed in graphite to form lithium-carbon compounds, expressed as follows: $6\text{C} + x\text{Li}^+ + xe^- \rightarrow \text{C}_6\text{Li}_x$. Simultaneously, the electrons at the cathode side pass through the external circuit to the anode. The discharge process is the opposite: lithium ions are released by the lithium-carbon compound and return to the cathode, with the electrons flowing from the anode to the cathode through the external circuit.

Based on the energy storage mechanisms, supercapacitors can be classified into two types: electric double-layer capacitors involving electrostatic adsorption/desorption on the surface of active materials,^[15] and pseudocapacitors based on rapid reversible surface redox reactions.^[16]

The energy storage process of double-layer capacitors mainly depends on the electric double layer formed at the interface between each electrode and the electrolyte. As illustrated in Figure 2b, when an external voltage is applied to both electrodes of the supercapacitor, the anions and cations in the electrolyte migrate to the anode and the cathode, respectively, and form a double layer on the surface of the corresponding electrodes. After the electric field is withdrawn,

the positive and negative charges on the electrodes attract the oppositely charged ions present in the electrolyte solution; thus, the electric double layers are stable and a relatively stable voltage is generated between the electrodes. This type of a capacitor has high power density and excellent cycle performance.

Pseudocapacitance, also known as Faraday quasi-capacitance, is the capacitance produced by highly reversible chemisorption, desorption, or oxidation and reduction reactions occurring at the electrodes.^[17] It is the main mechanism of energy storage in metal oxide, metal carbide, and conductive polymer supercapacitors. Compared to a double-layer capacitor, a pseudocapacitor has a higher energy density. However, owing to the electrochemical reaction kinetics and the irreversibility of the reaction, the charging and discharging power and cycle life of a pseudocapacitor are less than those of a double-layer capacitor.

An MIHC is assembled using battery- and capacitor-type counter electrodes. It has mainly two configurations: metal anode//carbon cathode and battery-type material (anode/cathode)//carbon (cathode/anode). The ion storage mechanism of a metal anode//carbon cathode configuration (e.g., activated carbon (AC) cathode//Zn anode) is as follows.^[10a] On the Zn anode, during the charge-discharge process, mainly the stripping/plating of Zn/Zn^{2+} occurs ($\text{Zn} \leftrightarrow \text{Zn}^{2+} + 2e^-$). On the AC cathode, Zn^{2+} cation and SO_4^{2-} anion adsorption/desorption occurs on the AC surface at different charge/discharge potentials. In comparison, in a typical $\text{MnO}_2/\text{ZnSO}_4$ (aq)//AC device,^[10c] the Zn^{2+} ions in the electrolyte flow to the anode under the effect of the electric field, and intercalation/de-intercalation occurs in MnO_2 during the charging process. Concurrently, SO_4^{2-} ions are adsorbed on the AC surface,

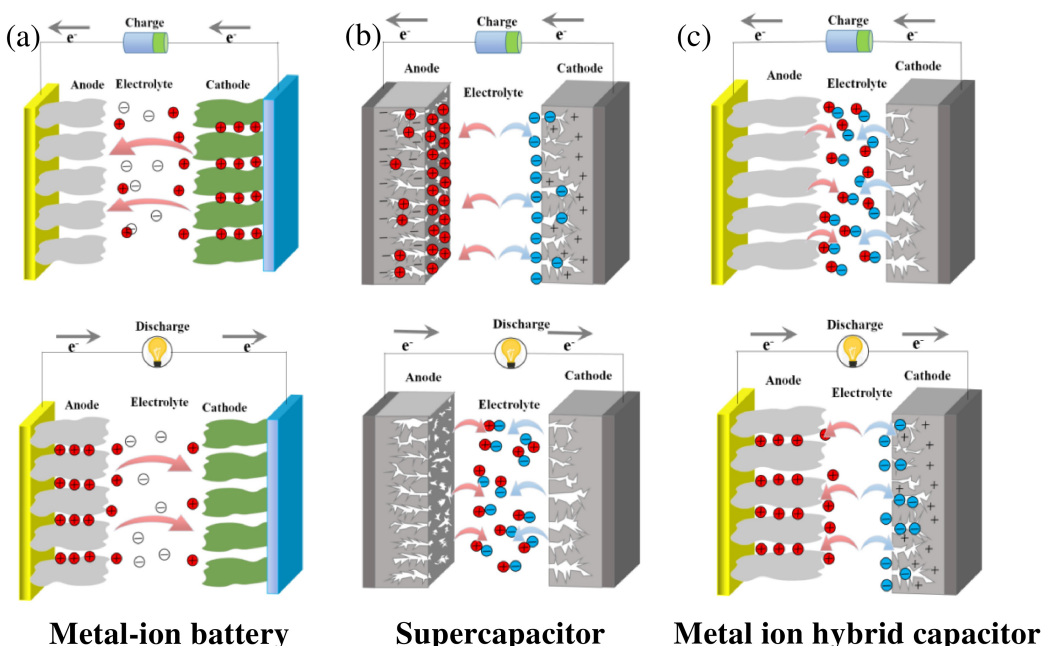


Figure 2. Illustration of the electrochemical mechanisms of different energy storage devices. a) Metal-ion battery. b) Supercapacitor. c) Metal-ion hybrid capacitor.

forming an electric double layer. The discharge process is the opposite; the Zn^{2+} ions in MnO_2 and the SO_4^{2-} ions on the AC surface flow from the electrode to the electrolyte. Some side reactions occur, such as the formation/dissolution of $Zn_4(OH)_6SO_4 \cdot nH_2O$ on both the MnO_2 cathode and the AC anode, which also contribute to the total capacitance of the device.

2.2. Zinc-Ion Hybrid Capacitor

In recent years, research has focused on ZHCs because of their low cost, high safety, environmental friendliness, and good electrochemical performance.^[18] In addition, the zinc electrode has a very high theoretical capacity (823 mAh g^{-1}) and low redox potential (-0.76 V) relative to the standard hydrogen electrode.^[19] However, the large-scale applications of ZHCs still require more in-depth research.^[20] Generally, ZHC devices consist of battery- and capacitor-type electrodes and an aqueous/organic/ionic liquid electrolyte. Based on the assembly forms, ZHC configurations can be classified into two types: carbon (phosphorene) cathode//Zn anode and metal oxide (sulfide)//carbon. In these, carbon typically acts as a capacitor-type electrode depending on the adsorption and desorption mechanism for energy storage. Currently, the effective approaches for improving the energy density of carbon materials are doping and surface modification.^[10a,21] The cathode can be zinc metal or other “beyond carbon” battery-type material, such as a metal oxide/sulfide/nitride.^[22] Moreover, the aqueous/organic electrolyte plays an important role in improving the Zn striping/plating efficiency in ZHC devices, increasing the reaction rate. The ionic conductivity of the electrolyte affects the capacity and performance of these devices.^[10a,22b, 23]

2.2.1. Capacitor-Type Materials for ZHCs

The most commonly used capacitor-type electrodes are carbon-based materials; however, the adsorption/desorption mechanisms of typical carbon materials significantly limit their capacitance. Thus, exploring new capacitor-type materials and improving the electrochemical performance of the existing carbon-based electrodes have become the focus in the development of high-performance ZHCs. Among these strategies, designing carbon-based capacitor-type materials with effective morphology and microstructure is a good approach to solve the problems of insufficient energy density and low capacity of ZHCs. The main methods are pore-making, doping, and surface modification.^{[18], [24]} Herein, carbon, modified carbon, and some other “beyond carbon” capacitor-type materials^[25] are summarized as follows.

2.2.1.1. Carbon Materials

Pan et al. synthesized two-dimensional (2D) multi-carbon porous nanosheets with large surface areas and adjustable

mesopore contents by a one-step $KHCO_3$ activation process.^[26] They used mild $KHCO_3$ as an activator to create nanopores in the carbon material, and the nanopores played a role in improving the electrochemical performance. As shown in Figure 3, PCNF-4 has an amorphous structure and numerous nanopores on its surface. The corresponding ZHC device presented considerable energy and power densities of 142.2 Wh kg^{-1} (0.5 A g^{-1}) and 15390 W kg^{-1} , respectively. The maximum capacity reached 177.7 mAh g^{-1} (0.5 A g^{-1}), and the rate performance and the cycle stability were reflected in the 90% retention rate after 10,000 cycles at 10 A g^{-1} .

Li et al. developed a pencil-shaving-derived porous carbon cathode material with a porous structure and a high specific surface area.^[27] The PSC-A600 cathode-based ZHC displayed excellent electrochemical performance. The specific capacity/capacity reached 413.3 F g^{-1} at 0.2 A g^{-1} , and a high retention rate of 92.2% was realized after 10,000 cycles at a high current density of 10 A g^{-1} . Furthermore, high power and energy densities of 15.7 kW kg^{-1} and 65.4 Wh kg^{-1} , respectively, were achieved. When PSC-A600 is used in conjunction with a particular antifreeze hydrogel electrolyte, a flexible ZHSC can be obtained and operates normally at a relatively lower temperature (-15°C).

Chen et al. constructed ZHCs with hollow mesoporous carbon nanospheres as electrical-grade materials (Figure 4).^[28] The hollow mesoporous structure with a high specific surface area realized rapid ion movement and easy adsorption/desorption. This distinct structure was used in both carbon cathodes and zinc anodes to improve Zn^{2+} electroplating/peeling. The corresponding ZHC device demonstrated high capacity (212.1 F g^{-1} at 0.2 A g^{-1}), excellent energy density (75.4 Wh kg^{-1} at 0.16 kW kg^{-1}), and excellent cycle stability (99.4% retention after 2500 cycles at a current density of 2 A g^{-1}).

Some examples of other carbon-based capacitor-type materials used in ZHCs are as follows: (i) a layered porous carbon with a three-dimensional (3D) interconnect structure (with a capacity of 305 mAh g^{-1} at 0.1 A g^{-1} , an energy density of Wh kg^{-1} , and 94.9% cycle retention after 20000 cycles at 2 A g^{-1}),^[29] (2) a flexible diamond fiber (with 89.9% cycle retention after 10,000 cycles at 1 A g^{-1}),^[30] and (3) high-density 3D graphene gels (with a specific capacity of 222.03 F g^{-1} at 0.5 A g^{-1} and 80% cycle retention after 30,000 cycles at 10 A g^{-1}).^[31]

2.2.1.2. Modified Carbon Materials

By doping carbon cloth (CC) with N and O atoms, Deng et al. developed a graded porous carbon, which was used as the cathode in a ZHC (Figure 5).^[32] This specific structure provides not only a high specific surface area but also more active sites and high conductivity owing to the doping of N and O atoms. Additionally, the structure combines H^+ and Zn^{2+} with C–O bonds and N–O bonds via chemical adsorption, thereby providing double cations (H^+ and Zn^{2+}), which participate in the reaction and increase the capacity of the system. The

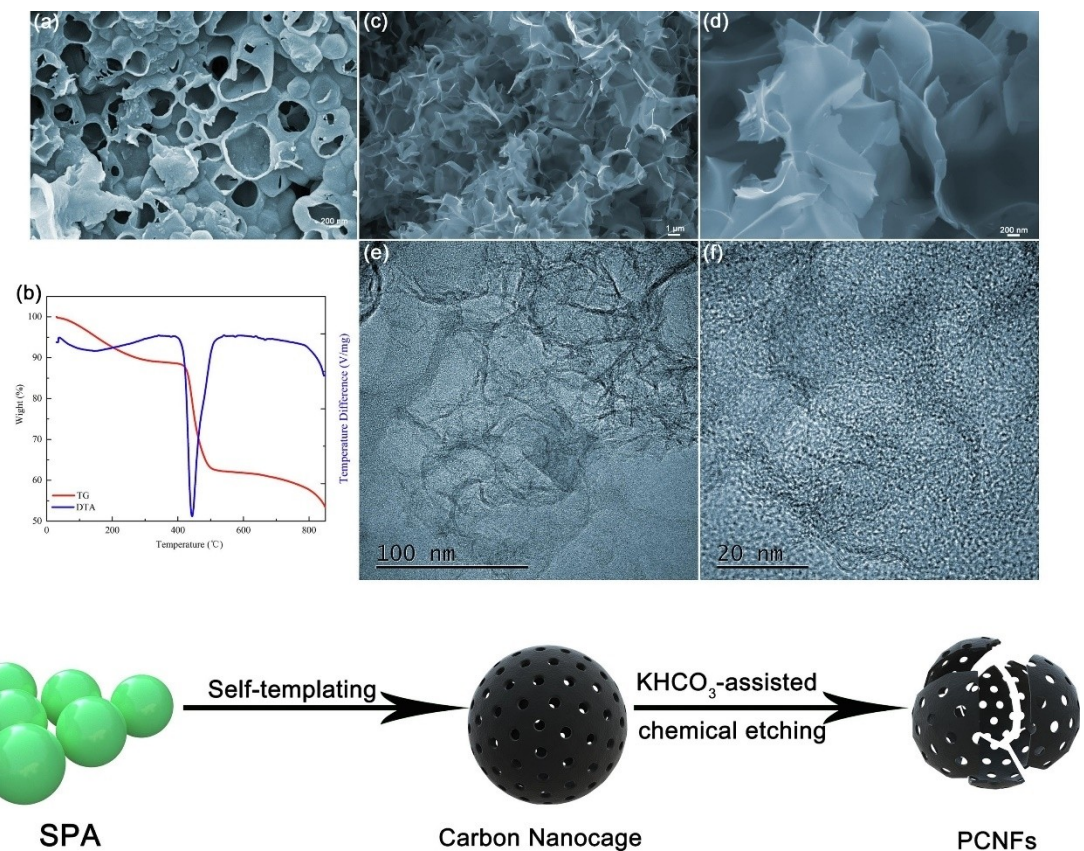
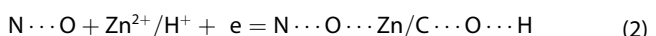
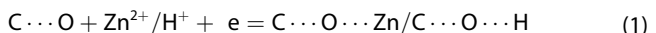


Figure 3. a, c–d) FESEM image of PCNF-0 and PCNF-4. b) TG-DTA image of THE SPA. e) TEM image of PCNF-4. f) HRTEM image of PCNF-4. g) Formation of PCNF. Reproduced from Ref. [26] with permission. Copyright (2020) Elsevier.

chemical adsorption/desorption process is expressed as follows [Eqs. (1) and (2)]:



The corresponding ZHC achieved a capacity of 138.5 mAh g⁻¹ at 0.5 A g⁻¹, with the energy density reaching 110 Wh kg⁻¹ and the power density being 20 kW kg⁻¹. Owing to their excellent performance, N,O-doped carbon cathodes are feasible solutions for ZHCs.

Some other doped carbon-based materials that can be used as ZHC capacitor-type electrodes are S-doped 3D porous carbon (providing a capacity of 203.3 mAh g⁻¹ at 0.2 A g⁻¹ and maintaining a 96.8% cycle retention after 18000 cycles),^[24b] polydopamine layered porous carbon cloth (the maximum area capacity is 1.25 mAh cm⁻², and a 100% retention rate is achieved after 10,000 cycles),^[33] and graphene nanosheet-manganese sulfide (with specific capacitance of 792 F g⁻¹, energy density of 25 Wh kg⁻¹, power density of 7.16 kW kg⁻¹, and 91% retention rate after 15,000 cycles).^[34]

2.2.1.3. “Beyond Carbon” Capacitor-Type Materials

By electrochemical stripping, Huang et al. prepared FL-P from black phosphorus (BP) as a cathode material for a ZHC (Figure 6).^[25] Phosphorus as a cathode material can effectively use carbon as a cathode material for overcoming the problem of low output voltage. Using an organic electrolyte, the output voltage of the abovementioned ZHC can be increased to 2.5 V, and the self-discharge problem can be reduced. The device composed of FL-P presents a high energy density of 315.6 Wh kg⁻¹ and a power density of 23.5824 kW kg⁻¹ and has good cycle stability. Certainly, this new type of cathode material broadens the prospect for ZHCs.

Wang et al. designed a new flexible ZHC based on a δ-MnO₂@CAC battery-type cathode and an MXene@COC capacitor-type anode in an aqueous liquid electrolyte (Figure 6, Figure 7). The “beyond carbon” MXene material exhibits excellent electrochemical behavior: a high energy density of 90 Wh kg⁻¹ at a power density of 239 W kg⁻¹, capacitance retention of ~80.7% after 16,000 cycles, and a high Coulomb efficiency exceeding 93.6% in all the cycles. Furthermore, the corresponding FZIC also presents good electrochemical performance while retaining its high flexibility.^[35]

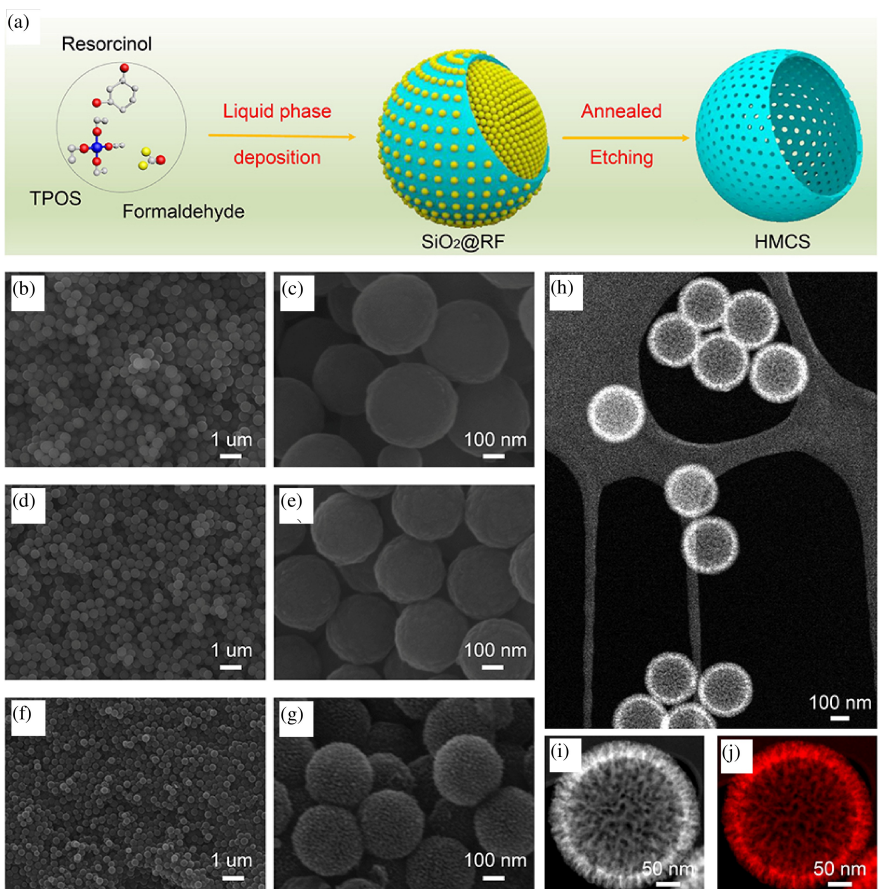


Figure 4. a) Manufacturing process of hollow mesoporous carbon nanospheres. b, c) SiO_2 carbon nanosphere intermediate. d, e) After carbonizing the organic surface, SiO_2 carbon nanosphere intermediate. f, g) Carbon nanosphere. h) HAADF image. i) STEM image. j) C-K edge elemental mapping. Reproduced from Ref. [28] under the terms of the Creative Commons License. Copyright (2020) The Authors.

2.2.2. Battery-Type Materials for ZHC

Depending on the two typical types of ZHC configurations, battery-type electrodes are mainly formed of zinc foil, zinc-based composites, and some “beyond zinc” materials.

2.2.2.1. Zinc Metal Electrode

As reported, the standard potential of the zinc metal electrode (vs. the standard hydrogen electrode) is as low as -0.76 V , which ensures a high working voltage for ZHCs. Additionally, the theoretical gravimetric and volumetric capacities are $\sim 823\text{ mAh g}^{-1}$ and 5845 Ah L^{-1} , respectively. Furthermore, Zn metal is stable in air, which suggests that Zn-based ZHCs are safer than univalent alkali-based hybrid capacitors. More importantly, Zn metal is abundant in nature, cost-effective, and non-toxic. However, there are also some problems with a Zn metal electrode, such as zinc dendrite growth in aqueous solution, which results in unstable cycling^[36]. Stable cycling is promoted when the device is tested in neutral or slightly acidic electrolytes (e.g., ZnSO_4 aqueous solution).^[10a,23a,37]

2.2.2.2. Zinc Composite Materials

Zinc is deposited on various substrates to reduce the growth of zinc dendrites. For example, Yang et al. deposited Zn nanosheets on diamond fibers, as shown in Figure 8, and a corresponding ZNC with a diamond/carbon fiber cathode and a Zn/diamond anode was built.^[24j] This device delivers an energy density of 70.7 Wh kg^{-1} at a power density of 709.0 W kg^{-1} . The electrochemical performance is sustained even at severe bending states.

Zn metal-based battery-type electrodes deposited on carbon cloth, carbon spheres, and other substrates have also been reported, which also exhibit excellent performance.^[38]

Feng et al. reported a Zn-ion hybrid micro-capacitor based on an AC cathode and a Zn nanosheet battery-type anode, as illustrated in Figure 9.^[39] The micro-device achieves a high capacitance of 259.4 F g^{-1} at a current density of 0.05 A g^{-1} , and the energy density reaches $115.4\text{ }\mu\text{Wh cm}^{-2}$ at 0.16 mW cm^{-2} . Benefiting from the electrodeposited Zn nanosheet anode, the cycling stability is excellent, remaining $\sim 100\%$ after 10000 cycles.

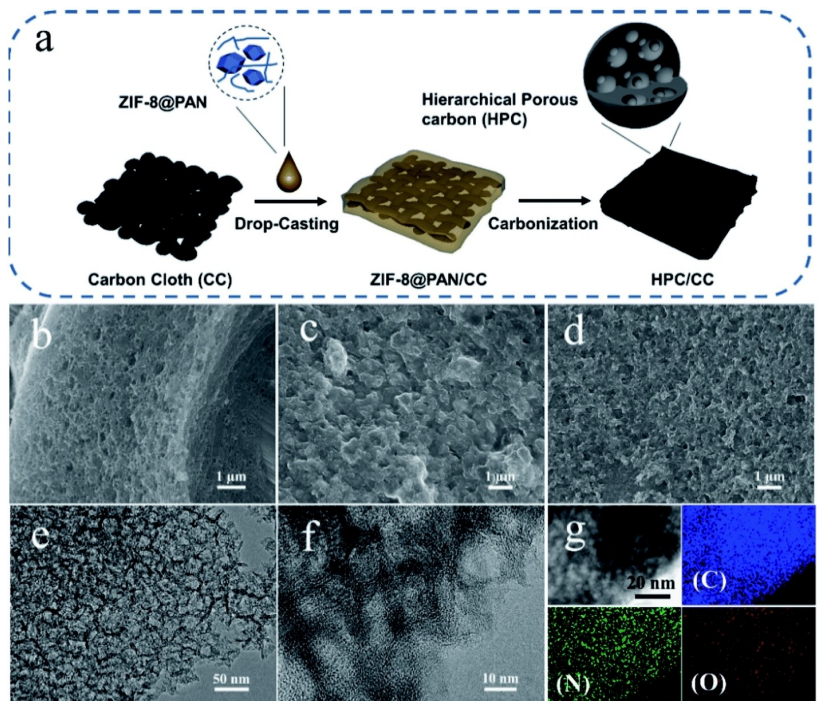


Figure 5. a) Schematic diagram of HPC/CC formation. b) and c) are the SEM images of HPC/CC-7 and HPC/CC-9, respectively. e-f) TEM images. g) Elements mapping of HPC/CC. Reproduced from Ref. [32] with permission. Copyright (2020) Royal Society of Chemistry.

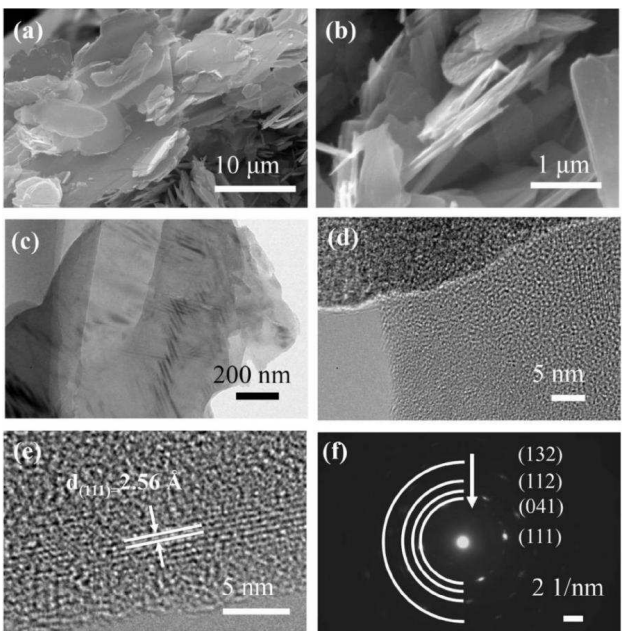


Figure 6. a–b) SEM images of FL-P. c–d) TEM images of FP-L. e) HRTEM image of FL-P. f) SAED images of FL-P. Reproduced from Ref. [25] with permission. Copyright (2020) Wiley-VCH.

2.2.2.3. Beyond Zinc Battery-Type Materials

Since the use of metallic zinc as the anode material of zinc batteries will cause a series of problems, such as the growth of zinc dendrites, etc.,^[22a,40] the use of other non-metallic zinc anode materials is a direction to solve these problems.

Although the use of other materials as the anode of a zinc ion battery can avoid the defects introduced by metallic zinc, it also introduces other problems.

A 2D layered TiS_2 was prepared to effectively solve the zinc dendrite growth problem. A ZHC was constructed using a TiS_2 battery-type anode and an AC capacitor-type cathode in ZnSO_4 electrolyte (Figure 9, Figure 10). The device presents a high specific capacitance of 249 F g^{-1} at 0.2 A g^{-1} and high energy and power densities of 112 Wh kg^{-1} , 3600 W kg^{-1} , respectively.^[41]

Metal oxides, such as MnO_2 , have also been employed as high-performance battery-type materials. As shown in Figure 11, an MnO_2 nanorods// ZnSO_4 (aq)//AC configuration ZHC was fabricated. The capacity of the device reached 54.1 mAh g^{-1} , and the energy density was as high as 34.8 Wh kg^{-1} . The high capacitance is mainly ascribed to the following mechanism: reversible insertion/extraction of Zn^{2+} cations into/from the MnO_2 battery-type material, SO_4^{2-} anion adsorption/desorption on the AC capacitor-type material, as well as some reversible side reactions, such as $\text{Zn}_4(\text{OH})_6\text{SO}_4 \cdot n\text{H}_2\text{O}$ formation on both electrodes.^[10c] Some other battery-type materials, such as MnS and VS_4 , which demonstrate good electrochemical performance, can be considered in ZHCs.^[42]

2.2.3. Electrolytes for ZHC

The selection of the electrolyte for ZHCs has been extensive. Zn-based salts in aqueous/organic liquids are commonly used

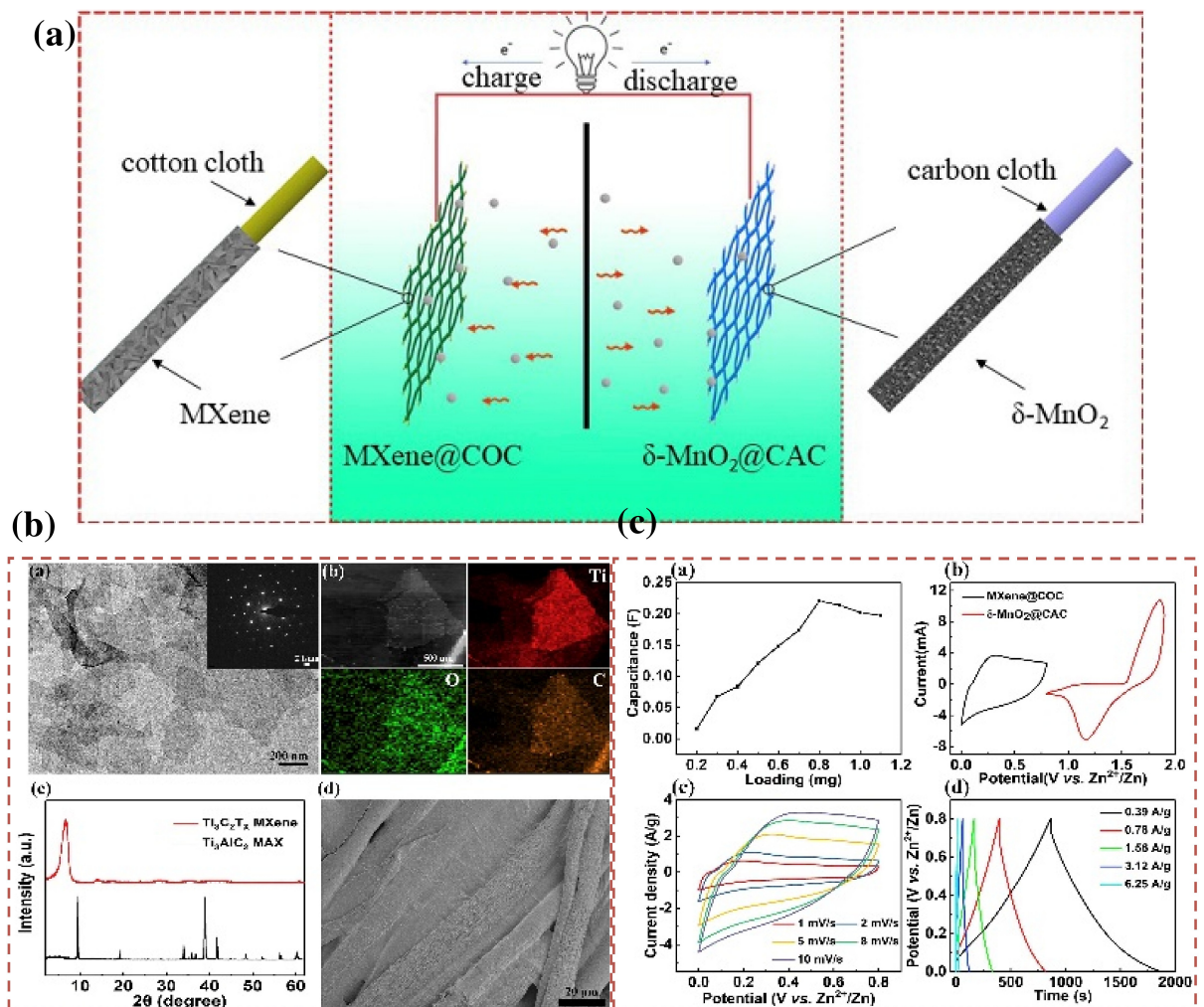


Figure 7. a) Schematic diagram of ZIC. b) The morphology of MXene@COC anode. c) Electrochemical performance display of MXene@COC anode. Reproduced from Ref. [35] with permission. Copyright (2019) Elsevier.

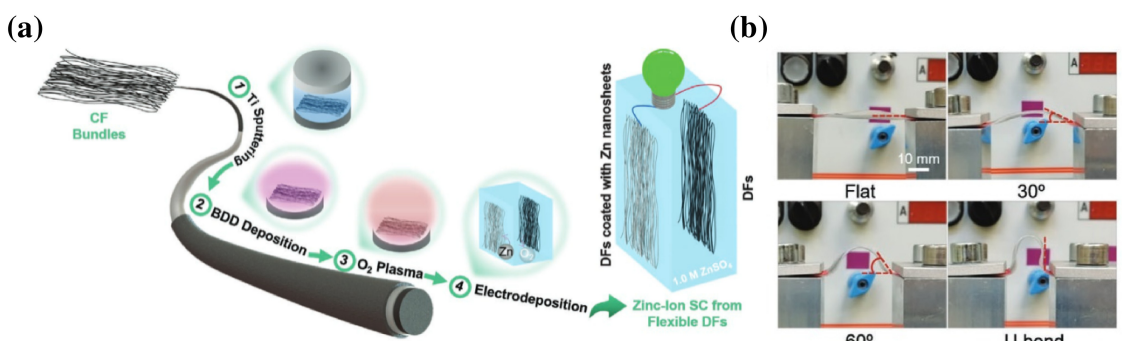


Figure 8. a) Schematic illustration of the synthesis of flexible DFs and the fabrication of zinc-ion SCs. b) Photographs of the SCs at different bending stage. Reproduced from Ref. [24j] under the terms of the Creative Commons License. Copyright (2020) The Authors.

as ZHC electrolytes.^[6a,18i,27–28,43] However, in recent years, numerous novel types of electrolytes, such as ionic liquids, have been reported to improve the performance of ZHCs.^[44]

2.2.3.1. Aqueous Electrolytes

In recent years, the researches of ZHCs' aqueous electrolyte has emerged in endlessly. Aqueous electrolyte has been the mainstream of ZHCs' electrolyte. Aqueous electrolytes are basically divided into two categories. One is the traditional

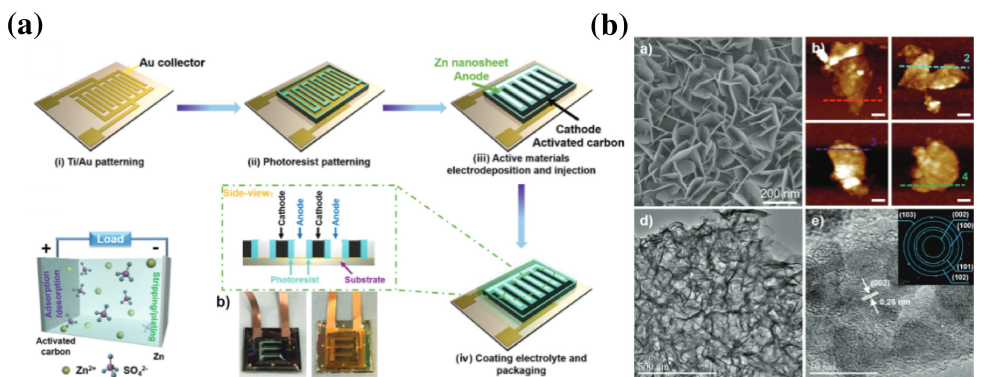


Figure 9. a) Schematic of the fabrication process of Zn-ion hybrid MSCs. b) Characterizations of electrodeposited Zn nanosheets as anode materials. Reproduced from Ref. [39] with permission. Copyright (2018) Wiley-VCH.

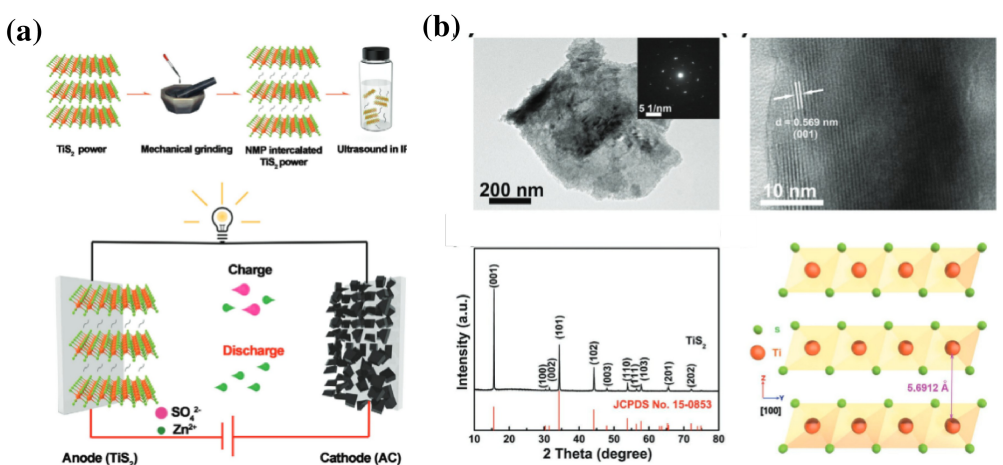


Figure 10. a) The fabricating process of TiS₂, and the structure and storage mechanism of the novel TiS₂//AC ZHSC. b) Morphology and structure of TiS₂. Reproduced from Ref. [41] with permission. Copyright (2020) Wiley-VCH.

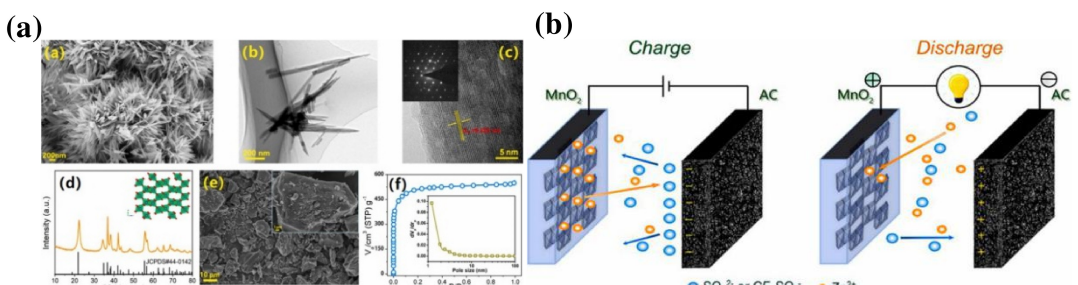


Figure 11. a) Structure and morphology of the synthesized MnO₂ nanorods. b) Schematic illustration of the designed aqueous MnO₂//AC ZHCs. Reproduced from Ref. [10c] with permission. Copyright (2018) Elsevier.

aqueous electrolyte which dissolve the zinc-base salt in water, such as ZnCl₂ or ZnSO₄ aqueous solution. And the other one is mixture of organic substance and water as the solvent which can improve the transport rate of zinc ions in the solution or can provide more ions to the redox reaction occurring on the cathode and anode. The following part will respectively introduce the typical examples of two kinds of ZHCs' aqueous electrolyte.

Aqueous electrolytes are the conventional ZHC electrolytes. In a typical ZHC device,^[43b] a Zn-base aqueous electrolyte (e.g., ZnCl₂, ZnSO₄, and Zn(CF₃SO₃)₂) is sandwiched between a zinc foil used as the anode and a porous carbon (aMEGO) derived from chemically activated graphene, used as the cathode. In this study, Zn(CF₃SO₃)₂, as a Zn-based material, was used as the aqueous electrolyte (Figure 12). The operating voltage window of the ZHC increased significantly to the range of 0–1.9 V because of the suppression of hydrogen and oxygen evolution.

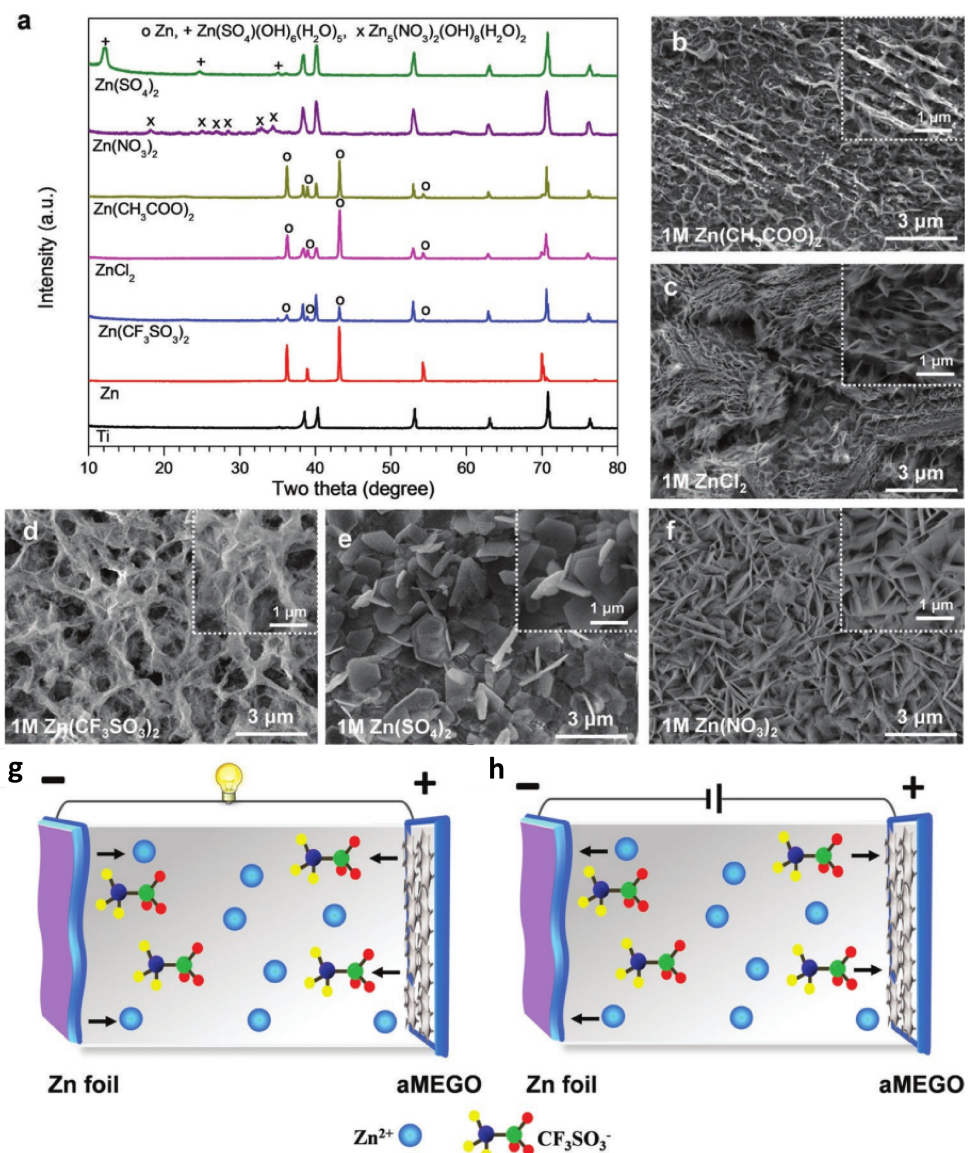


Figure 12. a) The XRD graph of Ti substrates with Zn layer plated in different Zn-based salts. b–f) The SEM images of Ti substrates with Zn layer plated in different Zn-based electrolytes. g, h) Schematic of charging/discharging process of the Zn-aMEGO hybrid capacitor. Reproduced from Ref. [43b] with permission. Copyright (2019) Wiley-VCH.

Therefore, its power density was 31.4 kW kg^{-1} and energy density reached 106.3 Wh kg^{-1} . The capacity remained 93% after 80000 cycles at a high current density.^[43b]

Some solid cellulose hydrogel electrolytes were developed. Han *et al.* reported a novel type of ZHC (Figure 13)^[45] In which an ionic natural polymer hydrogel was used as the electrolyte. In the capacitor, a sodium alginate (SA) electrolyte was sandwiched between AC serving as the cathode and a Zn foil acting as the anode. In a natural polymer backbone, acroleic acid and acrylamide were introduced to synthesize a hydrogel with a double-layer network by in situ free-radical polymerization.

An ethylene glycol/Zn-based salt ($ZnSO_4$)-based aqueous electrolyte was reported in 2020. The advantage of this novel hybrid electrolyte is its good performance at low temperature, e.g., the corresponding ZHC presented a high energy density

of 36 Wh kg^{-1} , a power density of 3.1 kW kg^{-1} , and a long-cycle life of 5500 cycles over 110 days at a temperature of -20°C .^[28]

A novel biodegradable cellulose hydrogel electrolyte based on $ZnCl_2$ was reported^[47]. The corresponding device displayed a wide electrochemical potential window and excellent ion conductivity, resulting in a high energy density of 192 Wh kg^{-1} . The flexible ZHC also presented excellent stability and can operate at a low temperature of -20°C .

2.2.3.2. Organic Electrolytes

ZHCs based on organic electrolytes were developed. Organic carbon//Zn ZHCs were also studied. $Zn[(CF_3SO_3)_2N]_2$ dissolved in organic solvents, such as acetonitrile (AN)^[10e] or a dimethyl ether (DME)/1,3-dioxolane (DOL) mixture,^[9c] were reported for

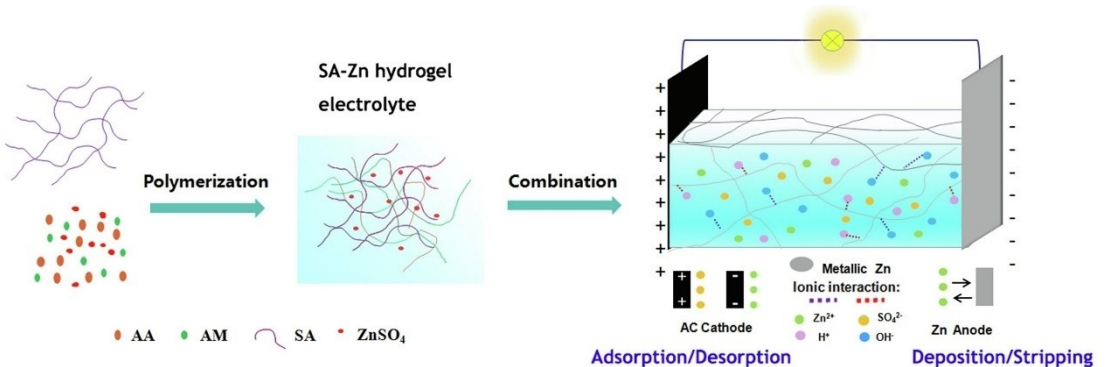


Figure 13. Schematic of the synthesis route and ionic interaction of H-ZHS. Reproduced from Ref. [45] with permission. Copyright (2019) Elsevier.

ZHCs. Tang *et al.* reported a porous carbon//Zn ZHC device using an organic electrolyte of $\text{Zn}[(\text{CF}_3\text{SO}_2)_2\text{N}]_2$ in DME/DOL.^[9c] The device demonstrated an excellent high discharge capacitance of 170 F g^{-1} at 0.1 A g^{-1} ; its energy/power density was as high as 52.7 Wh kg^{-1} at 1725 W kg^{-1} , and the capacity remained $\sim 91\%$ after 20,000 cycles at 2 A g^{-1} . Yoo *et al.* assembled an AC fiber (ACF)//Zn ZHC device based on a $\text{Zn}[(\text{CF}_3\text{SO}_2)_2\text{N}]_2$ /AN electrolyte.^[10e] The device displayed a wide working voltage range, high reversible capacity of $\sim 55 \text{ mAh g}^{-1}$ at a current of 5 mA cm^{-2} , and high capacity retention of $\sim 98\%$ after 10000 cycles, demonstrating good cyclic behavior.

2.2.3.3. Ionic Liquid Electrolytes

Ionic liquid electrolytes are characterized by good ionic conductivity, stable thermal and chemical properties, safety,

wide working voltage, and non-flammability. Ionic liquid electrolytes have been used in various energy storage systems, such as secondary batteries and supercapacitors. Liu *et al.* assembled a graphite//Zn ZHC device based on a biodegradable ionic liquid as the electrolyte.^[44a] The electrolyte was composed of Zn(OAc)_2 solute in a solvent mixture of choline acetate (70 wt%) and water (30 wt%). The ionic liquid electrolyte based ZHC device delivered high energy and power densities of 53 Wh kg^{-1} and 42 Wh kg^{-1} , respectively, and the capacitance remained $\sim 86\%$ after 1000 cycles at 0.5 A g^{-1} .

The Table 1 is a summary of some of the materials and electrochemical properties of zinc ion hybrid capacitors.

Overall, it is believed that ZHCs will have a wide range of applications in the future. However, more in-depth research should be conducted, e.g., the mechanism of energy storage, mechanism of interaction between the cathodes, anodes, and

Table 1. Materials and electrochemical properties of ZHSC.

Cathode	Anode	Electrolyte	Capacity	Cycle retention	Energy density [Wh kg ⁻¹]	Power density [kW kg ⁻¹]	Ref.
PCNF-4	Zn foil	$\text{ZnSO}_4(\text{aq})$	177.7 mAh g^{-1} (0.5 A g^{-1})	90% after 10000 cycles	142.2	15.39	[26]
PSC-A600	Zn foil	$\text{Zn}(\text{CF}_3\text{SO}_3)_2$	183.7 mAh g^{-1} (0.2 A g^{-1})	92.2% after 10000 cycles	147.0	15.7	[27]
HMCS	Zn	$\text{ZnSO}_4(\text{aq})$	212.1 F g^{-1} (0.2 A g^{-1})	99.4% after 2500 cycles	75.4	16.0	[28]
HPC	Zn	$\text{ZnSO}_4(\text{aq})$	305 mAh g^{-1} (0.1 A g^{-1})	94.9% after 20000 cycles	118	3.2	[29]
S-3DPCs	Zn foil	$\text{ZnSO}_4(\text{aq})$	203.3 mAh g^{-1} (0.2 A g^{-1})	96.8% after 18000 cycles	162.6	16.0	[24b]
DFs	SC	$\text{ZnSO}_4(\text{aq})$	35 F g^{-1} (0.2 A g^{-1})	89.9% after 10000 cycles	16.2	4.395	[30]
DGH	Zn foil	$\text{ZnSO}_4(\text{aq})$	222.03 F g^{-1} (0.5 A g^{-1})	80% after 30000 cycles	118.42 Wh L^{-1}	24 kW L^{-1}	[31]
HPC/CC	Zn foil	$\text{ZnSO}_4(\text{aq})$	138.5 mAh g^{-1} (0.5 A g^{-1})	100% after 10000 cycles	110	20	[32]
PDA/PCC	Zn/CC	$\text{ZnSO}_4(\text{aq})$	0.92 mAh cm^{-2}	100% after 10000 cycles	9.7 mWh cm^{-3}	–	[33]
PCNs-2	Zn	$\text{ZnSO}_4(\text{aq})$	149 mAh g^{-1} (0.2 A g^{-1})	91% after 10000 cycles	60	15.976	[47]
FL-P	Zn	PC	363.9 F g^{-1} (0.5 A g^{-1})	–	315.6	23.582	[25]
MnS	ZnS	KCL(aq)	884 F g^{-1} (2 mV s^{-1})	100% after 5000 cycles	91	7.78	[48]
MnO_2	MXene	–	–	80.7% after 16000 cycles	90	3.838	[35]
AC	Zn	$\text{ZnSO}_4(\text{aq})$	–	91% after 10000 cycles	30	14.9	[38]
MCHs/CC/PTFE	Zn/MCHs	Zn-Ion(aq)	–	–	–	–	[30]
TiS2	NPC	$\text{ZnSO}_4(\text{aq})$	249 F g^{-1} (0.2 A g^{-1})	–	28.6	0.1	[41]
Porous carbon	Zn/Carbon	–	–	87.6% after 10000 cycles	82.36	–	[24j]
AC	MnO_2	–	–	93.4% after 5000	34.8	–	[49]
BMM-9-900	MOF	–	–	98.5% after 1000 cycles	–	–	[50]
AC	Zn nanosheet	–	1297 mF cm^{-2}	100% after 10000 cycles	$115.4 \mu\text{Wh cm}^{-2}$	0.16 mW cm^{-2}	[39]
aMEGO	Zn foil	$\text{Zn}(\text{CF}_3\text{SO}_3)_2(\text{aq})$	823 mAh g^{-1}	93% after 80000 cycles	106.3	31.4	[43b]
AC	Zn foil	SA(aq)	–	95.4% after 2000 cycles	286.6	220	[51]
–	–	EG, $\text{ZnSO}_4(\text{aq})$	–	–	36	3.1	[28]
–	–	cellulose hydrogel	–	–	192	16.976	[46]

electrolyte, and development of more suitable electrode materials should be studied.

2.3. Magnesium-Ion Hybrid Capacitor

Magnesium ions have potentially important roles in both capacitors and batteries because of their abundant resources, stable chemical properties, and high theoretical capacity (3833 Ah L^{-1}).^[52] As summarized in Table 2, MHCs are mainly assembled in Mg//carbon and other battery-type materials//carbon configurations.^[10e,53] MHCs are also developing rapidly, despite the magnesium ion storage mechanism still remaining indistinct. Furthermore, more suitable electrode materials demand exploitation. The development of MHCs is summarized as follows.^[54]

2.3.1. Battery-Type Materials

2.3.1.1. Magnesium Metal

A magnesium foil can be used as a battery-type anode for magnesium ion supercapacitors. During the charging and discharging process, the magnesium foil is dissolved in the electrolyte, and the magnesium ions in the electrolyte are deposited on the anode. However, the electrolyte easily forms a passivation film on the anode. To solve this problem, researchers are still searching for new materials. Magnesium ion batteries (MIBs) are also facing this problem, and some solutions have been proposed. Bi and Sn compounds were studied as the anodes of MIBs; they can be highly compatible with most electrolytes.^[6c] Therefore, some similar metal compounds, such as those of Bi/Mg, can be considered as new battery-type materials for MHCs in the future.

Other battery-type materials of MIBs can be considered as the candidate materials for supercapacitor cathodes. For example, copper current collector-assisted tellurium.^[55] Ultrafine Te powder, super P, and CMC were mechanically mixed to form an electrode, which displayed high specific capacity (265.4 mAh g^{-1} at 2 A g^{-1}), long cycle stability time, and high rate performance, which were better than those of other materials previously reported.^[55]

2.3.1.2. "Beyond Magnesium" Battery-Type materials

There are many types of cathode materials for MHCs. MnO_2 is a promising electrode material because it has a high theoretical capacitance and a large potential window in a high-power energy storage capacitor.^[56] As shown in Figure 14, Liu et al. studied the electrochemical behavior of an MnO_2 electrode in a MgSO_4 electrolyte to deepen the understanding of an MHC.^[5c]

Varying the potential window affects the charge storage kinetics of Mg^{2+} ions on the MnO_2 electrode. When the starting voltage is positive, the oxidation-reduction reaction of the MnO_2 electrode is weak. The electrochemical characteristics are the best when the equilibrium potential window (0–1.2 V) is used to synthesize an $\text{MnO}_2@\text{CNTs}$ electrode. The MHC has a specific capacitance of 967 F g^{-1} at 10 mV s^{-1} , and the capacitance retention rate is 60%. The MgSO_4 electrolyte is also one of the reasons for the high capacitance and high retention rate of the capacitor; it accelerates the reaction efficiency and morphological changes of the MHC.

2.3.2. Capacitor-Type Materials

In the device models of MHCs, the mainly used capacitor-type material is carbon. Some carbon-based capacitor-type materials, such as AC,^[57] carbon aerogels^[6c] and ACF cloth,^[6c] have been reported. However, the adsorption/desorption mechanism of a typical carbon significantly limits its capacitance. Thus, exploring new capacitor-type materials and improving the electrochemical performance of carbon-based electrodes are also important for developing high-performance MHCs.

2.3.3. Electrolytes for MHC

The electrolytes of MHCs can be simply classified into inorganic and organic electrolytes. Examples of inorganic electrolytes are MgSO_4 and MgCl_2 .^[57] As an example, a modified ethereal-Mg organo-haloaluminate complex was used as the electrolyte of an MHC.^[6c] During the discharging process, Mg^{2+} ions accumulate on the ACF cloth, and the Mg foil also dissolves in the electrolyte. During the charging process, Mg^{2+} ions are ejected from the ACF surface. Researchers tested the potential

Table 2. Electrode materials and electrochemical performances of different MHCs and MIBs.

Electrode materials	Anode	Electrolyte	Electrochemical performance			Ref.
Cathode MHCs			Voltage [V]	Capacity	Capacity retention	
MnO_2	Mg	MgSO_4	0~1.2	580 F g^{-1}	60% scan rate 200 mVs	[5c]
Mg-based graphite	AC	$(\text{TFSI})_2\text{Pry}_{14}\text{TFSI}$	4.2~4.5	87 mAh g^{-1}	–	[57]
ACF cloth with a BET	Mg foil	$\text{Mg}_2\text{Cl}_3^{+}\text{-Ph}_2\text{AlCl}_2^{-}$	0.9~2.4 V	90 F g^{-1}	79% after 4500 cycles	[6c]
Carbon aerogels	Mg foil	$\text{Mg}_2\text{Cl}_3^{+}\text{-Ph}_2\text{AlCl}_2^{-}$	–	–	–	[6c]
MIBs						
Mg_2Ga_5	Mg	APC	–	290 mAh g^{-1}	922.5 mAh g^{-1} after 1000 cycles	[58]
Te-Cu	Mg	B-based Mg salts	0~0.19	118.8 mAh g^{-1}	$1119.2 \text{ mAh cm}^{-3}$ after 400 cycles	[55]
graphite fluoride	Mg	APC	–	813 mAh g^{-1}	–	[59]

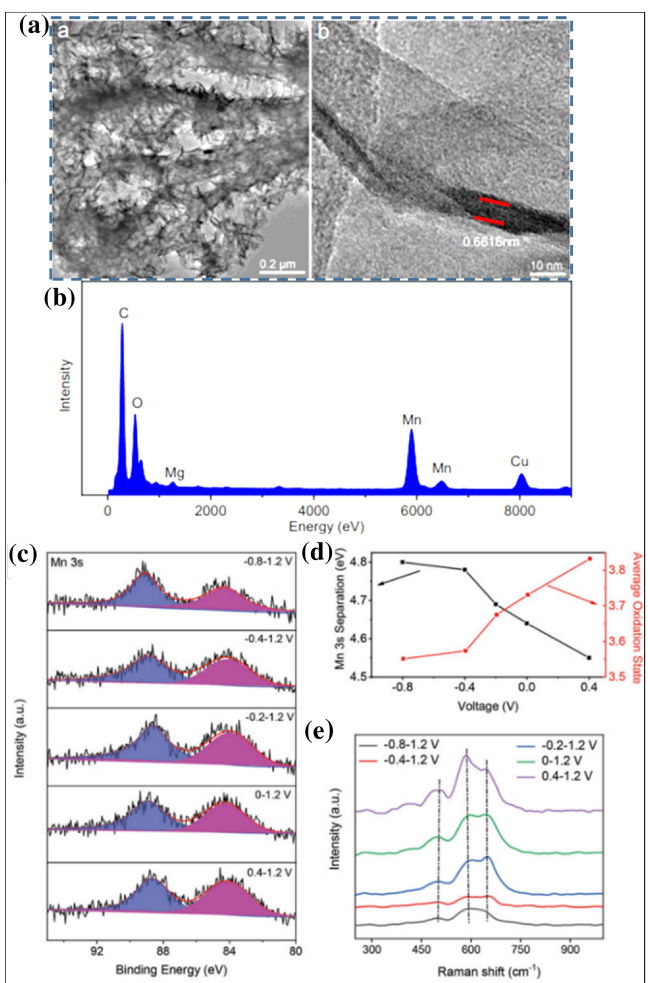


Figure 14. a) TEM image, b) energy dispersive X-ray spectrum, c) XPS spectra of MnO_2 @CNTs in Mn3S under different potentials; d) The average oxidation state of sample Mn under different potential window cycles; e) Raman spectra under different potential window cycles. Reproduced from Ref. [5c] with permission. Copyright (2019) Elsevier.

distributions of the cathode and the anode under various charge and discharge currents, and proposed that the dissolution and deposition rate of magnesium is relatively fast, which is sufficient to match the cathode.

2.4. Calcium-Ion Hybrid Capacitor

Calcium was considered to be a potential alternative to substitute traditional hybrid capacitor materials because of its abundant resources (it is the fifth most abundant element in the earth's crust) and high volume capacity (approximately 2073 mAh cm^{-3}).^[60] However, the use of calcium remains challenging, e.g., the reversibility of calcium metal anodes is poor owing to the formation of a passivation layer during the oxidation reaction of calcium ions. The recent progress of CHC research is described as follows.^[10d,61]

2.4.1. Battery-Type Materials

The direct use of metallic calcium anodes is far from meeting the performance requirements of commercial batteries, particularly in the low-power mode, which exhibits a low Coulomb efficiency. Most calcium energy storage devices use Sn as the battery-type electrode.^[10d] During the reaction, Sn reacts with Ca to form a Ca-Sn alloy (Ca_7Sn_6) (Figures 14a–c). When the alloy reacts, the electrons show rapid transmission characteristics.

Some battery-type materials used in calcium-ion batteries can be considered as CHC cathodes. In 2019, Liu et al. reported the successful synthesis of one-dimensional $\text{CaV}_6\text{O}_{16}$ ^[63] (Figure 15d). The material has a high capacity of 205 mAh g^{-1} at 0.3 C and retains 97% of its capacity after 200 cycles. Recently, phosphate compounds ($\text{Na}_2\text{FePO}_4\text{F}$)^[64] have been proposed as materials for cathodes of calcium-ion batteries. $\text{VOPO}_4 \cdot 2\text{H}_2\text{O}$ has a working potential as high as 2.8 V and its reversible capacity (Figure S23) is as high as 100.6 mAh g^{-1} .^[62]

2.4.2. Capacitor-Type Materials

Capacitor-type materials with large surface areas are required to meet the fast absorption/desorption of calcium ions. AC is typically used as a capacitor-type material dependent on the absorption/desorption mechanism.^[10d] Graphite-based materials have proven difficult to react at room temperature.^[65] However, recent studies have shown^[66] that when graphite is intercalated with dimethylacetamide, a stable reversible capacity over 200 cycles can be achieved. In addition, in the test of lithium

Table 3. Electrode materials and electrochemical performances of different CHCs and CIBs.

Electrode materials		Electrolyte	Electrochemical performance		Ref.	
Cathode	Anode		Voltage [V]	Capacity	Capacity retention	
CHCs						
AC	Sn	$\text{Ca}(\text{PF}_6)_2$	1.5–4.8	92 mAh g^{-1}	84 % after 1000 cycles	[10d]
CIBs						
–	Stainless Steel	$\text{Ca}(\text{BH}_4)_2\text{EC:PC}$	–	–	85 %	[61a]
–	–	$\text{Ca}(\text{BH}_4)_2\text{ THF}$	–	–	95 %	[69]
–	–	$\text{Ca}[\text{B}(\text{hfip})_4]_2 \cdot 4\text{DME}$	–	–	80 %	[10c]
Ca_xCuHCF	polyaniline	$\text{Ca}(\text{NO}_3)_2$	–	130 mAh g^{-1}	95 % after 200 cycles	[70]
Ca	Au	$\text{Ca}(\text{BH}_4)_2\text{LiBH}_4\text{-THF}$	–	170 mAh g^{-1}	99.1 %	[68]

batteries, MXene can provide a high voltage similar to AC, which shows greater potential as a negative electrode material.^[67]

2.4.3. Electrolytes for CHC

The electrolytes used for aqueous Calcium-Ion Battery is mainly $\text{Ca}(\text{NO}_3)_2$. Lee, C. etc. reported that its molar ratio is about 1:7.5 ($\text{Ca}(\text{NO}_3)_2$:water molecule). According to this ratio, 97% of the initial energy can still be maintained after 150 cycles.^[67] Unlike other metal capacitors, Ca^{2+} is easy reacting with SO_4^{2-} , CO_3^{2-} and OH^- . The precipitate will make the capacitor performance sharply reduced.

In the study of non-aqueous electrolytes, it has been reported that $\text{Ca}(\text{BH}_4)_2$ can achieve reversible calcium metal coating/peeling at high temperatures. However, because of its needs for high temperature, low efficiency, and short cycle life, it still needs improvement. Recently, $\text{Ca}(\text{PF}_6)_2$,^[10d] $\text{Ca}[\text{B}(\text{hfp})_4]_2 \cdot 4\text{DME}$,^[10c] and $\text{Ca}(\text{BH}_4)_2 \cdot \text{LiBH}_4 \cdot \text{THF}$ were reported,^[68] which effectively weakened the solvation effect of Ca^{2+} at

room temperature and maintained high performance after many cycles. In particular, the Coulombic efficiency of $\text{Ca}(\text{BH}_4)_2 \cdot \text{LiBH}_4 \cdot \text{THF}$ reached 99.1% (Figure 16)

In summary, although calcium ions have natural advantages in calcium ion hybrid capacitors, the following more research is needed to promote its practical application: 1. Exploration of better electrolytes to accelerate the reaction speed of calcium and improve the Coulomb efficiency. 2. Developing more high-performance electrode materials, such as calcium and other metal alloys.

2.5. Aluminum-Ion Hybrid Capacitors (AHCs)

Aluminum is one of the most important elements in the Earth's crust. It has unique three-electron redox characteristics,^[71] as expressed in Equation (3). Its specific capacity and volume capacity were as high as 2980 mAh g^{-1} and 8046 mAh cm^{-3} , respectively. Therefore, AHCs have received increased attention. Table 4 summarizes the relevant research progress of AHCs:^[10b,72]

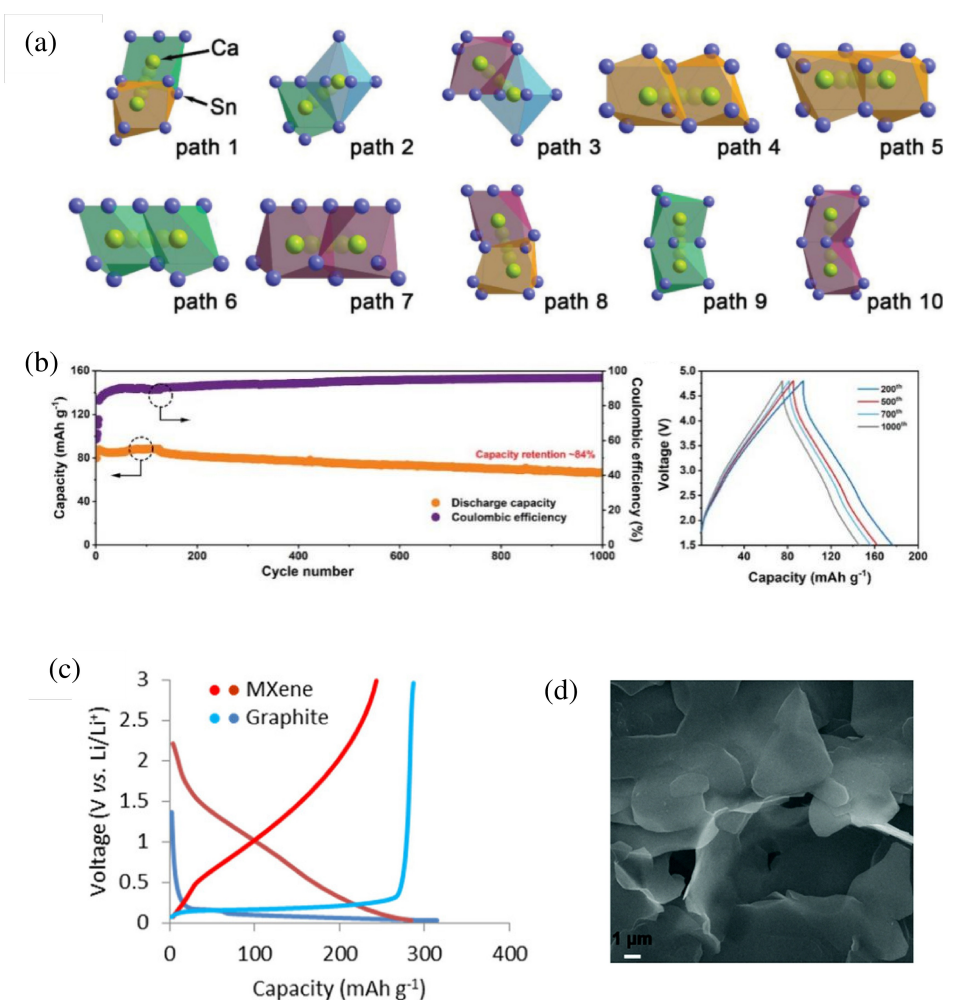


Figure 15. a) evolution of Ca in Ca_2Sn_8 . b) Capacitor cycle test curve. c) MXene and graphite voltage test in lithium battery. Reproduced from Ref. [10d] with permission. Copyright (2019) Wiley-VCH. d) $\text{VOPO}_4 \cdot 2\text{H}_2\text{O}$ microscopic image. Reproduced from Ref. [62] under the terms of the Creative Commons License. Copyright (2020) The Authors.

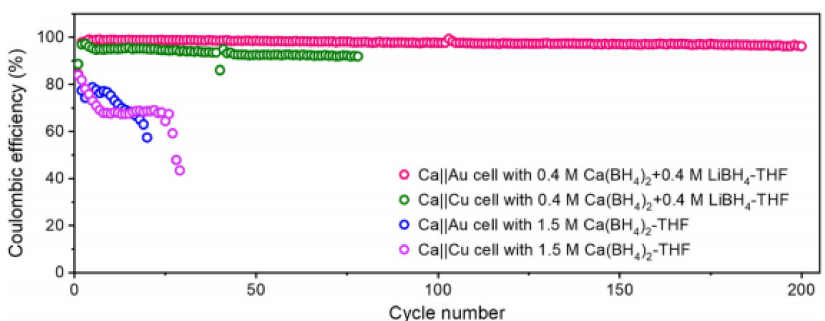


Figure 16. CE values of $\text{Ca}(\text{BH}_4)_2\text{-LiBH}_4\text{-THF}$. Reproduced from Ref. [68] with permission. Copyright (2020) Wiley-VCH.

Table 4. Electrode materials and electrochemical performances of different AHCs and AlBs.

Electrode materials	Electrochemical performance			Ref.		
Cathode AHCs	Anode	Electrolyte	Voltage [V]	Capacity	Capacity retention	
CuFe-PBA	AC	$\text{Al}(\text{NO}_3)_3$	0–0.8	50 mAh g^{-1}	90% after 1000 cycles	[75]
AC	$\text{MoO}_3@\text{PPy}$	$\text{Al}_2(\text{SO}_4)_3$	0–1.5	$140 \text{ mAh g}^{-1} (1 \text{ A g}^{-1})$	~93% after 1800 cycles	[72]
SCNT/(PANI)	SCNT/ $\text{W}_{18}\text{O}_{49}$	AlCl_3	0–1.8	–	95.9% after 6000 cycles	[10b]
P-TiO ₂ -MRs	AC	AlCl_3	0–1.9	$49.8 \text{ mAh g}^{-1} (5 \text{ A g}^{-1})$	63% after 1000 cycles	[9b]
AlBs						
N-3PC	Al	AlCl_3	0.1–2.2	$33 \text{ mAh g}^{-1} (500 \text{ mA g}^{-1})$ $17 \text{ mAh g}^{-1} (1 \text{ A g}^{-1})$	8 mAh g^{-1} after 20 cycles (2 A g^{-1})	[74]
Mo_6S_8	Al	AlCl_3 and $[\text{BMIm}] \text{Cl}$	–	$40 \text{ mAh g}^{-1} (60 \text{ mA g}^{-1})$ $25 \text{ mAh g}^{-1} (120 \text{ mA g}^{-1})$	70 mAh g^{-1} after 50 cycles (6 mA g^{-1})	[78]
WS ₂ (2D)	Al	AlCl_4^-	–	$254 \text{ mAh g}^{-1} (0.1 \text{ A g}^{-1})$ $86 \text{ mAh g}^{-1} (5 \text{ A g}^{-1})$	119 mAh g^{-1} after 500 cycles (1 A g^{-1})	[80]



2.5.1. Capacitor-Type Materials

Thus far, the capacitor materials for AHCs have mainly comprised carbon. One type of such materials are carbon-based materials. Owing to the excellent work of Dai and his co-workers in 2015,^[73] graphite, 3D graphite foam, graphene aerogel, carbon nanotubes, as well as the current nitrogen-doped porous carbons^[74] can all be used as the cathode of aluminum ion batteries (AlBs).

2.5.2. Battery-Type Materials

$\text{K}_{0.02}\text{Cu}[\text{Fe}(\text{CN})_6]_{0.7} \cdot 3.7\text{H}_2\text{O}$,^[75] MoO_3 ,^[72] $\text{W}_{18}\text{O}_{49}$,^[10b] TiO_2 ,^[9b] and conductivity polymers^[72] have been reported for AHC devices. Wang et al. used MoO_3 nanotubes coated with conducting PPy ($\text{MoO}_3@\text{PPy}$) as the anode in an $\text{AC}/\text{Al}_2(\text{SO}_4)_3$ (aq)/ $\text{MoO}_3@\text{PPy}$ AHC device. The effective working range of this capacitor is 0–1.5 V, and its capacity can still be maintained above 90% after more than 1800 charge-discharge cycles, which is very excellent.^[72] A novel SCNT/polystyrene (PANI)/ $\text{Al}_2(\text{SO}_4)_3$ (aq)/SCNT/ $\text{W}_{18}\text{O}_{49}$ AHC was studied. The device exhibited good stability and high flexibility; the energy and power densities were as high as 19.0 mWh cm^{-3} and 295 mW cm^{-3} ,^[10b] respec-

tively, and the reaction mechanism for charge storage is expressed in Equation (4). Furthermore, in a recent breakthrough, an AHC with a porous TiO_2 microrod (P-TiO₂-MRs) battery-type electrode was synthesized. It can achieve an energy density of 26.3 Wh kg^{-1} at 627.3 W kg^{-1} and a good power density of 5454.5 W kg^{-1} at 10.9 Wh kg^{-1} (Figure 17). Its excellent performance may be attributed to the following: Compared to ordinary nanoparticles, the P-TiO₂-MRs material has a higher density, which enables better contact between the electrode and the electrolyte and improves the performance.^[9b] Additionally, polypyrrole and polythiophene have been proven to have relatively high electrochemical voltage plateaus when applied as battery-type electrodes in AHCs.^[76] The synthesized triangular phenanthrene-quinone-based macrocyclic compound electrodes with redox activity also exhibit good electrochemical performance.



Other battery-type materials used in AlBs, such as transition metal oxygen/sulfide TiO_2 ,^[77] V_2O_5 ,^[12d] Mo_6S_8 ,^[78] MoS_2 ,^[79] and WS₂ microchips,^[80] can be considered as battery-type electrodes of AHC devices.

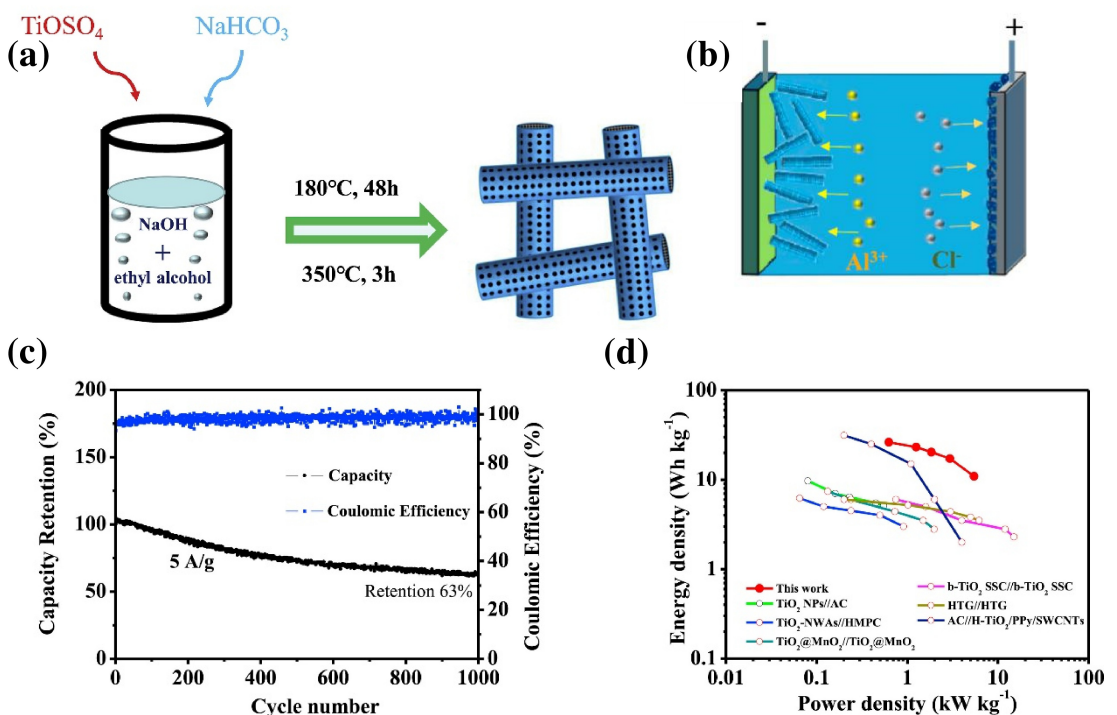


Figure 17. Some relevant information for the capacitor: a) The preparation process. b) The working mechanism. c) Long cycle stability at 5 A g^{-1} . d) Ragone plot of this capacitor. Reproduced from Ref. [9b] with permission. Copyright (2020) Elsevier.

2.5.3. Electrolytes for AHC

The electrolytes used for AHCs are mainly $\text{Al}(\text{NO}_3)_3$, $\text{Al}_2(\text{SO}_4)_3$, and AlCl_3 . We analyzed and listed the electrolytes used in AIBs. The use of salt-based electrolytes in water, such as AlCl_3 , will cause a series of adverse reactions, resulting in a low efficiency of the Al anode. Therefore, for non-aqueous electrolytes, relevant research and development has been conducted, mainly including molten salt electrolytes and room-temperature ionic liquid electrolytes. The former include the $\text{AlCl}_3\text{-NaCl}$ electrolyte and ternary $\text{AlCl}_3\text{/LiCl/KCl}$ electrolytes used in secondary AIBs, where the peeling/deposition process of Al follows Equation (5). The latter include 1-ethyl-3-methylimidazole chloride, 1-butyl-3methylimidazole chloride, and AlCl_3 . The stripping/deposition process of Al follows Equation (6). Molten salt electrolytes have limited AHC applications owing to their high melting point, and the use of expensive imidazole-based ionic liquid electrolytes for commercial use is evidently unrealistic. Low-cost alternative materials, such as a recently developed low-cost room temperature ionic liquid electrolyte mixed with $\text{AlCl}_3\text{-ethylamine hydrochloride}$,^[81] need to be explored intensively in the future. In addition to those listed above, there are solid polymer electrolytes,^[82] gel polymer electrolytes,^[83] and mixed electrolytes.^[84]



2.6. Conclusion and Outlook

In this paper, four types of MMHCs are summarized: calcium, magnesium, aluminum, and zinc ion-based devices. The design concept, electrochemical performance, material selection, and composition of the anode, cathode, and electrolyte of these four capacitors are introduced, respectively. In general, compared with conventional metal (ion) batteries and supercapacitors, MMHCs have evident advantages, such as simultaneous high energy density and high power density, ultra-long cycle life, safety, as well as more abundant multivalent metal resources. Although MMHCs have promising applications, certain challenges remain and some issues still need to be addressed, which are mainly described as follows:

The electrochemical reaction mechanisms of the multivalent ions in MMHC electrodes remain unclear. The ionic diameter, charge number, reactivity, ionic diffusion coefficient, and binding energy (between the ions and the active materials) of univalent and multivalent ions are completely different, which will induce different insertion-extraction dynamics in battery-type electrodes. Additionally, the electrochemical behavior of the multivalent ions in capacitor-type materials should not only be an ion adsorption/desorption mechanism. More effective and refined material characterization strategies and electrochemical measurements should be adopted. For example, in situ infrared spectroscopy, in situ X-ray diffraction, and X-ray photoelectron spectroscopy can be used to monitor the surface groups, phases, and chemical states of electrodes at various charge-discharge states. If necessary, theoretical calcu-

lations should be performed to understand the reaction dynamics.

More suitable active materials should be developed for high-performance MMHC devices. Currently, although ZHCs have received much attention, research related to CHCs, MHCs, and AHCs is rare. Thus, multivalent ion batteries based on Ca, Mg, and Al that correspond to the above-mentioned MMHCs need to be exploited, which will provide more materials to choose from. In particular, "beyond metal" electrodes for CHCs/MHCs/AHCs are important for developing novel "beyond metal"/carbon MMHC configurations. For the most studied ZHC devices, i. novel active carbon materials should be designed, such as preparing self-supporting carbon films to avoid conductive agents and binders. ii. Effective doping, defects, and modification need to be conducted. The introduction of appropriate sulfur/oxygen/nitrogen group defects and other surface modifications will significantly improve the capacitance of carbon by introducing more active sites, promoting conductivity, and improving affinity with the electrolyte. iii. The metal electrodes of MMHCs should be redesigned to reduce the total weight of the MMHC devices. For example, metal foams and metal-carbon composite nanomaterials can be utilized.

MMHCs with all-solid-state, flexible, wearable, miniature, and portable functions need to be developed. Because MMHC devices have demonstrated remarkable advantages, specific functions can be integrated to achieve wide commercial applications.

Acknowledgements

This project was financially supported by the "Guangdong Special Support Program" Science and Technology Innovation Youth Top Talent Project (No. 2019TQ05C578), Guangzhou Science and Technology Program (No. 202002030460), and Special Innovation Projects of Universities in Guangdong Province (No. 2017KTSCX057).

Conflict of Interest

The authors declare no conflict of interest.

Keywords: multivalent metal-ion hybrid capacitors • high-capacity cathodes • high energy density • electrolyte • energy storage

- [1] a) J. Hwang, K. Takeuchi, K. Matsumoto, R. Hagiwara, *J. Mater. Chem. A* **2019**, *7*, 27057–27065; b) C. Jo, A. S. Groombridge, J. De La Verpilliere, J. T. Lee, Y. Son, H. L. Liang, A. M. Boies, M. De Volder, *ACS Nano* **2020**, *14*, 698–707; c) P. J. Lian, B. S. Zhao, L. Q. Zhang, N. Xu, M. T. Wu, X. P. Gao, *J. Mater. Chem. A* **2019**, *7*, 20540–20557; d) P. W. Yuan, S. H. Guo, S. Q. Gao, J. Wang, W. Q. Chen, M. Li, K. Y. Ma, N. Wang, F. Liu, J. P. Cheng, *J. Alloys Compd.* **2019**, *780*, 147–155; e) L. Zhu, Z. L. Chen, Y. Song, P. Wang, Y. C. Jiang, L. Jiang, Y. N. Zhou, L. F. Hu, *Nanoscale* **2018**, *10*, 5581–5590.

- [2] a) L. N. Zhao, G. R. Chen, Y. H. Weng, T. T. Yan, L. Y. Shi, Z. X. An, D. S. Zhang, *Chem. Eng. J.* **2020**, *401*, 126138; b) Y. Sun, Q. L. Zou, Y. C. Lu, *Adv. Energy Mater.* **2019**, *9*; c) L. Fan, R. F. Ma, J. Wang, H. G. Yang, B. A. Lu, *Adv. Mater.* **2018**, *30*, 1903002; d) T. Danner, M. Singh, S. Hein, J. Kaiser, H. Hahn, A. Latz, *J. Power Sources* **2016**, *334*, 191–201.
[3] a) D. S. Mallapragada, N. A. Sepulveda, J. D. Jenkins, *Appl. Energy* **2020**, *275*, 115390; b) S. Wang, X. B. Zhang, *Adv. Mater.* **2019**, *31*, 1805432; c) P. F. Wang, Y. You, Y. X. Yin, Y. G. Guo, *Adv. Energy Mater.* **2018**, *8*, 1701912; d) G. Zou, C. Wang, H. Hou, C. Wang, X. Qiu, X. Ji, *Small* **2017**, *13*, 1700762.
[4] a) J. Cabana, L. Monconduit, D. Larcher, M. R. Palacin, *Adv. Mater.* **2010**, *22*, E170-E192; b) B. Dunn, H. Kamath, J. M. Tarascon, *Science* **2011**, *334*, 928–935; c) N. Nitta, F. X. Wu, J. T. Lee, G. Yushin, *Mater. Today* **2015**, *18*, 252–264; d) M. M. Thackeray, C. Wolverton, E. D. Isaacs, *Energy Environ. Sci.* **2012**, *5*, 7854–7863; e) X. R. Wang, G. Q. Tan, Y. Bai, F. Wu, C. Wu, *Electrochem. Energy Rev.* **2020**, <https://doi.org/10.1007/s41918-020-00073-4>; f) N. Yabuuchi, K. Kubota, M. Dahbi, S. Komaba, *Chem. Rev.* **2014**, *114*, 11636–11682.
[5] a) W. Czepa, S. Witomska, A. Ciesielski, P. Samori, *Nanoscale* **2020**, *12*, 18733–18741; b) Z. Y. Jing, S. J. Qi, X. Tao, H. L. Yu, W. Zhang, Y. L. Qiao, X. Y. Li, H. S. Dong, *J. Mater. Sci.* **2021**, *56*, 3296–3311; c) Y. P. Liu, Y. X. Zhang, Z. H. Sun, S. T. Cheng, P. Cui, Y. Wu, J. L. Zhang, J. C. Fu, E. Q. Xie, *Small* **2020**, *16*, 2003403; d) M. Marimuthu, S. Ganesan, J. Y. Johnbosco, *Electrochim. Acta* **2020**, *357*; e) Z. R. Zhang, Z. P. Yao, X. Zhang, Z. H. Jiang, *Electrochim. Acta* **2020**, *359*, 136848.
[6] a) L. B. Dong, W. Yang, W. Yang, H. Tian, Y. F. Huang, X. L. Wang, C. J. Xu, C. Y. Wang, F. Y. Kang, G. X. Wang, *Chem. Eng. J.* **2020**, *384*, 12335; b) P. Pazhamalai, K. Krishnamoorthy, S. Sahoo, S. J. Kim, *J. Alloys Compd.* **2018**, *765*, 1041–1048; c) L. B. Dong, W. Yang, W. Yang, Y. Li, W. J. Wu, G. X. Wang, *J. Mater. Chem. A* **2019**, *7*, 13810–13832; d) Y. S. Luo, D. S. Tsai, C. C. Wang, C. W. Chiang, *J. Phys. Chem. C* **2020**, *124*, 21909–21918.
[7] a) D. P. Dubal, K. Jayaramulu, J. Sunil, S. Kment, P. Gomez-Romero, C. Narayana, R. Zboril, R. A. Fischer, *Adv. Funct. Mater.* **2019**, *29*, 1900532; b) H. X. Li, J. T. Chen, L. Zhang, K. J. Wang, X. Zhang, B. J. Yang, L. Y. Liu, W. S. Liu, X. B. Yan, *J. Mater. Chem. A* **2020**, *8*, 16302–16311; c) H. X. Li, J. W. Lang, S. L. Lei, J. T. Chen, K. J. Wang, L. Y. Liu, T. Y. Zhang, W. S. Liu, X. B. Yan, *Adv. Funct. Mater.* **2018**, *28*.
[8] a) Y. C. Hu, Y. J. Yu, K. Huang, L. Wang, *J. Energy Storage* **2020**, *27*; b) G. Neumann, *Chem. Ing. Tech.* **2011**, *83*, 2042–2050; c) G. L. Zhu, C. Z. Zhao, J. Q. Huang, C. X. He, J. Zhang, S. H. Chen, L. Xu, H. Yuan, Q. Zhang, *Small* **2019**, *15*.
[9] a) P. A. Maughan, N. Tapia-Ruiz, N. Bimbo, *Electrochim. Acta* **2020**, *341*; b) X. C. Zhou, Y. Z. Lu, Y. C. Zhen, Z. Z. Wang, X. Y. Zheng, M. D. Wei, Z. S. Hong, *J. Power Sources* **2020**, *453*, 227857; c) H. Wang, M. Wang, Y. B. Tang, *Energy Storage Mater.* **2018**, *13*, 1–7.
[10] a) L. B. Dong, X. P. Ma, Y. Li, L. Zhao, W. B. Liu, J. Y. Cheng, C. J. Xu, B. H. Li, Q. H. Yang, F. Y. Kang, *Energy Storage Mater.* **2018**, *13*, 96–102; b) N. Li, Q. Yang, X. Liu, X. K. Huang, H. Y. Zhang, C. X. Wang, *ACS Appl. Mater. Interfaces* **2017**, *9*, 42093–42101; c) X. P. Ma, J. Y. Cheng, L. B. Dong, W. B. Liu, J. Mou, L. Zhao, J. J. Wang, D. Y. Ren, J. L. Wu, C. J. Xu, F. Y. Kang, *Energy Storage Mater.* **2019**, *20*, 335–342; d) N. Z. Wu, W. J. Yao, X. H. Song, G. Zhang, B. J. Chen, J. H. Yang, Y. B. Tang, *Adv. Energy Mater.* **2019**, *9*, 1803865; e) H. D. Yoo, S. D. Han, R. D. Bayliss, A. A. Gewirth, B. Genorio, N. N. Rajput, K. A. Persson, A. K. Burrell, J. Cabana, *ACS Appl. Mater. Interfaces* **2016**, *8*, 30853–30862.
[11] C. J. Xu, Y. Y. Chen, S. Shi, J. Li, F. Y. Kang, D. S. Su, *Sci. Rep.* **2015**, *5*, 14120.
[12] a) X. W. Yu, A. Manthiram, *Adv. Funct. Mater.* **2020**, *30*, 1805996; b) N. Li, X. Xu, B. W. Sun, K. Y. Xie, W. Huang, T. Yu, *Energy Storage Mater.* **2020**, *25*, 382–403; c) J. X. Wu, F. Ciucci, J. K. Kim, *Chem. Eur. J.* **2020**, *26*, 6296–6319; d) A. M. Diem, B. Fenk, J. Bill, Z. Burghard, *Nanomaterials* **2020**, *10*, 247; e) W. J. Song, S. Yoo, G. Song, S. Lee, M. Kong, J. Rim, U. Jeong, S. Park, *Batteries & Supercaps* **2019**, *2*, 181–199; f) C. S. Pan, R. X. Zhang, R. G. Nuzzo, A. A. Gewirth, *Adv. Energy Mater.* **2018**, *8*, 1800589; g) J. T. Herb, C. A. Nist-Lund, C. B. Arnold, *J. Mater. Chem. A* **2017**, *5*, 7801–7805; h) P. Canepa, G. S. Gautam, R. Malik, S. Jayaraman, Z. Q. Rong, K. R. Zavadil, K. Persson, G. Ceder, *Chem. Mater.* **2015**, *27*, 3317–3325.
[13] a) N. P. Deng, Y. Feng, G. Wang, X. X. Wang, L. Y. Wang, Q. X. Li, L. T. Zhang, W. M. Kang, B. W. Cheng, Y. Liu, *Chem. Eng. J.* **2020**, *401*, 125976; b) C. L. Zhu, D. M. Hu, H. Pan, H. Yuan, Y. Li, J. F. Mao, Z. P. Guo, Z. X. Chen, M. Imtiaz, S. M. Zhu, *Carbon* **2020**, *170*, 66–74; c) I. W. Ock, J. Lee, J. K. Kang, *Adv. Energy Mater.* **2020**, *10*, 2001851; d) K. J. Kim, M. Balaish, M. Wadaguchi, L. P. Kong, J. L. M. Rupp, *Adv. Energy Mater.* **2020**, *11*, 2002689; e) S. Chen, S. Fan, D. B. Xiong, M. E. Pam, Y. Wang, Y. M. Shi, H. Y. Yang, *Small* **2020**, *16*, 2005095 ; f) Y. M. Jeon, S. Kim, M.

- Lee, W. B. Lee, J. H. Park, *Adv. Energy Mater.* **2020**, *10*, 2003114; g) S. Bai, B. Kim, C. Kim, O. Tamwattana, H. Park, J. Kim, D. Lee, K. Kang, *Nat. Nanotechnol.* **2021**, *16*, 77–84; h) Q. Yang, Q. Li, Z. X. Liu, D. H. Wang, Y. Guo, X. L. Li, Y. C. Tang, H. F. Li, B. B. Dong, C. Y. Zhi, *Adv. Mater.* **2020**, *32*, 2001854; i) Y. Q. Cao, X. B. Meng, A. D. Li, *Energy Environ. Sci.* **2020**, <https://doi.org/10.1002/eem2.12132>; j) H. Y. Wu, S. Q. Zhou, C. H. Tseng, M. L. Qin, A. Shiue, A. M. Chu, Z. Q. Cao, B. R. Jia, X. H. Qu, *J. Am. Ceram. Soc.* **2020**, *104*, 1102–1109; k) C. Liang, X. Zhang, S. X. Xia, Z. Y. Wang, J. Y. Wu, B. Yuan, X. Luo, W. Y. Liu, W. Liu, Y. Yu, *Nat. Commun.* **2020**, *11*, 5367.
- [14] a) P. Novak, J. C. Panitz, F. Joho, M. Lanz, R. Imhof, M. Coluccia, *J. Power Sources* **2000**, *90*, 52–58; b) S. Al Hallaj, R. Venkatachalamapathy, J. Prakash, J. R. Selman, *J. Electrochem. Soc.* **2000**, *147*, 2432–2436; c) K. Park, S. Yu, C. Lee, H. Lee, *J. Power Sources* **2015**, *296*, 197–203; d) I. Yamada, K. Miyazaki, T. Fukutsuka, Y. Iriyama, T. Abe, Z. Ogumi, *J. Power Sources* **2015**, *294*, 460–464; e) V. Aravindan, Y. S. Lee, S. Madhavi, *Adv. Energy Mater.* **2015**, *5*; f) N. S. Hudak, L. E. Davis, G. Nagasubramanian, *J. Electrochem. Soc.* **2015**, *162*, A315–A321.
- [15] a) J. E. Stark, A. Allison, H. A. Andreas, *Carbon* **2020**, *170*, 245–255; b) G. C. Li, K. Mao, M. Liu, M. L. Yan, J. Zhao, Y. Zeng, L. J. Yang, Q. Wu, X. Z. Wang, Z. Hu, *Adv. Mater.* **2020**, *32*, 2004632; c) E. Senokos, M. Rana, M. Vila, J. Fernandez-Cestau, R. D. Costa, R. Marcilla, J. J. Vilatela, *Nanoscale* **2020**, *12*, 16980–16986; d) Q. Dou, H. S. Park, *Energy Environ. Mater.* **2020**, *3*, 286–305.
- [16] a) B. E. Conway, W. G. Pell, *J. Solid State Electrochem.* **2003**, *7*, 637–644; b) J. Park, C. W. Lee, J. H. Park, S. H. Joo, S. K. Kwak, S. Ahn, S. J. Kang, *Adv. Sci.* **2018**, *5*, 1801365; c) A. J. Perez, R. Beer, Z. F. Lin, E. Salager, P. L. Taberna, A. M. Abakumov, P. Simon, J. M. Tarascon, *Adv. Energy Mater.* **2018**, *8*, 1702855; d) J. Zhang, H. J. Feng, Q. Qin, G. F. Zhang, Y. X. Cui, Z. Z. Chai, W. J. Zheng, *J. Mater. Chem. A* **2016**, *4*, 6357–6367; e) X. M. Li, Q. G. Li, Y. Wu, M. C. Rui, H. B. Zeng, *ACS Appl. Mater. Interfaces* **2015**, *7*, 19316–19323; f) L. Huang, X. Gao, Q. Dong, Z. M. Hu, X. Xiao, T. Q. Li, Y. L. Cheng, B. Yao, J. Wan, D. Ding, Z. Ling, J. S. Qiu, J. Zhou, *J. Mater. Chem. A* **2015**, *3*, 17217–17223; g) Y. Jang, J. Jo, H. Jang, I. Kim, D. Kang, K. Y. Kim, *Appl. Phys. Lett.* **2014**, *104*, 243901.
- [17] a) J. Dong, Y. He, Y. L. Jiang, S. S. Tan, Q. L. Wei, F. Y. Xiong, Z. L. Chu, Q. Y. An, L. Q. Mai, *Nano Energy* **2020**, *73*, 104838; b) D. F. Ying, R. Ding, Y. F. Huang, W. Shi, Q. L. Xu, C. N. Tan, X. J. Sun, P. Gao, E. H. Liu, *J. Mater. Chem. A* **2019**, *7*, 18257–18266; c) J. Dong, Y. L. Jiang, Q. L. Wei, S. S. Tan, Y. A. Xu, G. B. Zhang, X. B. Liao, W. Yang, Q. D. Li, Q. Y. An, L. Q. Mai, *Small* **2019**, *15*, 1900379; d) F. Yu, Z. C. Liu, R. W. Zhou, D. M. Tan, H. X. Wang, F. X. Wang, *Mater. Horiz.* **2018**, *5*, 529–535; e) X. Wang, S. Kajiyama, H. Iinuma, E. Hosono, S. Oro, I. Moriguchi, M. Okubo, A. Yamada, *Nat. Commun.* **2015**, *6*, 6544; f) W. T. Gu, M. Sevilla, A. Magasinski, A. B. Fuertes, G. Yushin, *Energy Environ. Sci.* **2013**, *6*, 2465–2476.
- [18] a) W. Guo, C. Yu, S. F. Li, Z. Wang, J. H. Yu, H. W. Huang, J. S. Qiu, *Nano Energy* **2019**, *57*, 459–472; b) Y. Q. Fu, Q. L. Wei, G. X. Zhang, X. M. Wang, J. H. Zhang, Y. F. Hu, D. N. Wang, L. C. Zuin, T. Zhou, Y. C. Wu, S. H. Sun, *Adv. Energy Mater.* **2018**, *8*, 1801445; c) N. Zhang, L. Zhang, Z. X. Cheng, *Neural Information Processing (Iconip) 2017*, Pt III **2017**, *10636*, 405–415; d) F. Yu, L. Pang, X. X. Wang, E. R. Waclawik, F. X. Wang, K. Ostrivkov, H. X. Wang, *Energy Storage Mater.* **2019**, *19*, 56–61; e) Z. D. Huang, T. R. Wang, H. Song, X. L. Li, G. J. Liang, D. H. Wang, Q. Yang, Z. Chen, L. T. Ma, Z. X. Liu, B. Gao, J. Fan, C. Y. Zhi, *Angew. Chem. Int. Ed.* **2021**, *60*, 1011–1021; f) H. F. Li, L. T. Ma, C. P. Han, Z. F. Wang, Z. X. Liu, Z. J. Tang, C. Y. Zhi, *Nano Energy* **2019**, *62*, 550–587; g) Z. X. Liu, Q. Yang, D. H. Wang, G. J. Liang, Y. H. Zhu, F. N. Mo, Z. D. Huang, X. L. Li, L. T. Ma, T. C. Tang, Z. G. Lu, C. Y. Zhi, *Adv. Energy Mater.* **2019**, *9*, 1902473; h) H. Y. Ma, H. W. Chen, M. M. Wu, F. Y. Chi, F. Liu, J. X. Bai, H. H. Cheng, C. Li, L. T. Qu, *Angew. Chem. Int. Ed.* **2020**, *59*, 14541–14549; i) C. Wang, Z. X. Pei, Q. Q. Meng, C. M. Zhang, X. Sui, Z. W. Yuan, S. J. Wang, Y. Chen, *Angew. Chem. Int. Ed.* **2020**, *60*, 990–997; j) P. Zhang, B. Y. Guan, L. Yu, X. W. Lou, *Angew. Chem. Int. Ed.* **2017**, *56*, 7141–7145; *Angew. Chem.* **2017**, *129*, 7247–7251.
- [19] a) F. Wang, O. Borodin, T. Gao, X. L. Fan, W. Sun, F. D. Han, A. Faraone, J. A. Dura, K. Xu, C. S. Wang, *Nat. Mater.* **2018**, *17*, 543; b) Y. X. Zeng, X. Y. Zhang, R. F. Qin, X. Q. Liu, P. P. Fang, D. Z. Zheng, Y. X. Tong, X. H. Lu, *Adv. Mater.* **2019**, *31*, 1903675.
- [20] N. Choudhary, C. Li, J. Moore, N. Nagaiah, L. Zhai, Y. Jung, J. Thomas, *Adv. Mater.* **2017**, *29*, 1605336.
- [21] a) J. Wang, P. Nie, B. Ding, S. Y. Dong, X. D. Hao, H. Dou, X. G. Zhang, *J. Mater. Chem. A* **2017**, *5*, 2411–2428; b) P. G. Liu, Y. Gao, Y. Y. Tan, W. F. Liu, Y. P. Huang, J. Yan, K. Y. Liu, *Nano Res.* **2019**, *12*, 2835–2841.
- [22] a) W. C. Du, E. H. X. Ang, Y. Yang, Y. F. Zhang, M. H. Ye, C. C. Li, *Energy Environ. Sci.* **2020**, *13*, 3330–3360; b) K. E. K. Sun, T. K. A. Hoang, T. N. L. Doan, Y. Y. X. Zhu, Y. Tian, P. Chen, *ACS Appl. Mater. Interfaces* **2017**, *9*, 9681–9687; c) Y. H. Cui, Q. H. Zhao, X. J. Wu, Z. J. Wang, R. Z. Qin, Y. T. Wang, M. Q. Liu, Y. L. Song, G. Y. Qian, Z. B. Song, L. Y. Yang, F. Pan, *Energy Storage Mater.* **2020**, *27*, 1–8; d) A. Mitha, A. Z. Yazdi, M. Ahmed, P. Chen, *ChemElectroChem* **2018**, *5*, 2409–2418.
- [23] a) H. L. Pan, Y. Y. Shao, P. F. Yan, Y. W. Cheng, K. S. Han, Z. M. Nie, C. M. Wang, J. H. Yang, X. L. Li, P. Bhattacharya, K. T. Mueller, J. Liu, *Nat. Energy* **2016**, *1*, 16039; b) J. Fu, L. Li, D. Lee, J. M. Yun, B. K. Ryu, K. H. Kim, *Appl. Surf. Sci.* **2020**, *504*, 144250; c) K. V. Sankar, Y. Seo, S. C. Lee, S. C. Jun, *ACS Appl. Mater. Interfaces* **2018**, *10*, 8045–8056.
- [24] a) Y. G. Lee, G. H. An, *ACS Appl. Mater. Interfaces* **2020**, *12*, 41342–41349; b) D. W. Wang, S. Y. Wang, Z. M. Lu, *Int. J. Energy Res.* **2020**, *45*, 2498–2510; c) N. Fechler, G. A. Tiruye, R. Marcilla, M. Antonietti, *RSC Adv.* **2014**, *4*, 26981–26989; d) G. H. An, *Appl. Surf. Sci.* **2020**, *530*, 147220; e) B. D. Boruah, A. Mathieson, B. Wen, C. S. Jo, F. Deschler, M. De Volder, *Nano Lett.* **2020**, *20*, 5967–5974; f) Q. Wang, S. L. Wang, X. H. Guo, L. M. Ruan, N. Wei, Y. Ma, J. Y. Li, M. Wang, W. Q. Li, W. Zeng, *Adv. Electron. Mater.* **2019**, *5*, 1900537; g) J. Yin, W. L. Zhang, W. X. Wang, N. A. Alhebsi, N. Salah, H. N. Alshareef, *Adv. Energy Mater.* **2020**, *10*, 2001705; h) D. F. Ying, Q. L. Xu, R. Ding, Y. F. Huang, T. Yan, Y. X. Huang, C. N. Tan, X. J. Sun, P. Gao, E. H. Liu, *Chem. Eng. J.* **2020**, *388*, 124154; i) J. X. Zhao, H. Y. Li, C. W. Li, Q. C. Zhang, J. Sun, X. N. Wang, J. B. Guo, L. Y. Xie, J. X. Xie, B. He, Z. Y. Zhou, C. H. Lu, W. B. Lu, G. Zhu, Y. G. Yao, *Nano Energy* **2018**, *45*, 420–431; j) Z. Jian, N. J. Yang, M. Vogel, S. Leith, A. Schulte, H. Schönher, T. P. Jiao, W. J. Zhang, J. L. Müller, B. Butz, X. Jiang, *Adv. Energy Mater.* **2020**, *10*, 2002202; k) Y. C. Zhu, X. K. Ye, H. D. Jiang, J. X. Xia, Z. Y. Yue, L. H. Wang, Z. Q. Wan, C. Y. Jia, X. J. Yao, *J. Power Sources* **2020**, *453*, 227851.
- [25] Z. D. Huang, A. Chen, F. N. Mo, G. J. Liang, X. L. Li, Q. Yang, Y. Guo, Z. Chen, Q. Li, B. B. Dong, C. Y. Zhi, *Adv. Energy Mater.* **2020**, *10*, 2001024.
- [26] Z. M. Pan, Z. M. Lu, L. Xu, D. W. Wang, *Appl. Surf. Sci.* **2020**, *510*, 145384.
- [27] Z. W. Li, D. H. Chen, Y. F. An, C. L. Chen, L. Y. Wu, Z. J. Chen, Y. Sun, X. G. Zhang, *Energy Storage Mater.* **2020**, *28*, 307–314.
- [28] S. H. Chen, G. Q. Yang, X. J. Zhao, N. Z. Wang, T. T. Luo, X. Chen, T. C. Wu, S. J. Jiang, P. A. van Aken, S. L. Qu, T. Li, L. Du, J. Zhang, H. B. Wang, Y. Wang, *Front. Chem.* **2020**, *8*, 663.
- [29] P. F. Yu, Y. Zeng, Y. X. Zeng, H. W. Dong, H. Hu, Y. L. Liu, M. T. Zheng, Y. Xiao, X. H. Lu, Y. R. Liang, *Electrochim. Acta* **2019**, 327.
- [30] Z. Jian, N. J. Yang, M. Vogel, S. Leith, A. Schulte, H. Schönher, T. P. Jiao, W. J. Zhang, J. Müller, B. Butz, X. Jiang, *Adv. Energy Mater.* **2020**, *10*, 2002202.
- [31] L. Z. D. W. G. W. Y. X. H. L. X. Yan, *Chinese Chem. Lett.* . **2020**, doi.org/10.1016/j.ccl.2020.06.037.
- [32] X. Y. Deng, J. J. Li, Z. Shan, J. W. Sha, L. Y. Ma, N. Q. Zhao, *J. Mater. Chem. A* **2020**, *8*, 11617–11625.
- [33] C. Huang, X. Zhao, Y. L. Xu, Y. Zhang, Y. J. Yang, A. P. Hu, Q. L. Tang, X. Y. Song, C. Z. Jiang, X. H. Chen, *ACS Sustainable Chem. Eng.* **2020**, *8*, 16028–16036.
- [34] V. Vignesh, K. Subramani, M. S. Oh, M. Sathish, R. Navamathavan, *Mater. Chem. Phys.* **2019**, *230*, 249–257.
- [35] J. Shi, S. Wang, Q. Wang, X. Chen, X. Du, M. Wang, Y. Zhao, C. Dong, L. Ruan, W. Zeng, J. Power Sources **2020**, *446*, 227345.
- [36] a) Y. W. Shen, K. Kordesch, *J. Power Sources* **2000**, *87*, 162–166; b) A. A. Mohamad, *J. Power Sources* **2006**, *159*, 752–757.
- [37] a) C. J. Xu, B. H. Li, H. D. Du, F. Y. Kang, *Angew. Chem. Int. Ed.* **2012**, *51*, 933–935; *Angew. Chem.* **2012**, *124*, 957–959; b) D. Kundu, B. D. Adams, V. Duffort, S. H. Vajargah, L. F. Nazar, *Nat. Energy* **2016**, *1*, 16119.
- [38] P. G. Liu, W. F. Liu, Y. P. Huang, P. L. Li, J. Yan, K. Y. Liu, *Energy Storage Mater.* **2020**, *25*, 858–865.
- [39] P. P. Zhang, Y. Li, G. Wang, F. X. Wang, S. Yang, F. Zhu, X. D. Zhuang, O. G. Schmidt, X. L. Feng, *Adv. Mater.* **2019**, *31*, 1806005.
- [40] J. X. Zheng, Q. Zhao, T. Tang, J. F. Yin, C. D. Quilty, G. D. Renderos, X. T. Liu, Y. Deng, L. Wang, D. C. Bock, C. Jaye, D. H. Zhang, E. S. Takeuchi, K. J. Takeuchi, A. C. Marschilok, L. A. Archer, *Science* **2019**, *366*, 645.
- [41] Q. Wang, S. L. Wang, J. Y. Li, L. M. Ruan, N. Wei, L. S. Huang, Z. Y. Dong, Q. H. Cheng, Y. Xiong, W. Zeng, *Adv. Electron. Mater.* **2020**, *6*, 20000388.
- [42] a) X. J. Chen, W. Li, Y. B. Xu, Z. P. Zeng, H. C. Tian, M. Velayutham, W. Y. Shi, W. Y. Li, C. M. Wang, D. Reed, V. V. Khramtsov, X. L. Li, X. B. Liu, *Nano Energy* **2020**, *75*, 104869; b) W. B. Liu, J. W. Hao, C. J. Xu, J. Mou, L. B. Dong, F. Y. Jiang, Z. Kang, J. L. Wu, B. Z. Jiang, F. Y. Kang, *Chem. Commun.* **2017**, *53*, 6872–6874; c) H. G. Qin, Z. H. Yang, L. L. Chen, X. Chen, L. M. Wang, *J. Mater. Chem. A* **2018**, *6*, 23757–23765; d) Q. C. Zhu,

- Q. Xiao, B. W. Zhang, Z. C. Yan, X. Liu, S. Chen, Z. F. Ren, Y. Yu, *J. Mater. Chem. A* **2020**, *8*, 10761–10766.
- [43] a) L. He, Y. Liu, C. Y. Li, D. Z. Yang, W. G. Wang, W. Q. Yan, W. B. Zhou, Z. X. Wu, L. L. Wang, Q. H. Huang, Y. S. Zhu, Y. H. Chen, L. J. Fu, X. H. Hou, Y. P. Wu, *ACS Appl. Mater. Interfaces* **2019**, *2*, 5835; b) S. L. Wu, Y. T. Chen, T. P. Jiao, J. Zhou, J. Y. Cheng, B. Liu, S. R. Yang, K. L. Zhang, W. J. Zhang, *Adv. Energy Mater.* **2019**, *9*, 1902915; c) L. Han, H. L. Huang, J. F. Li, X. L. Zhang, Z. L. Yang, M. Xu, L. K. Pan, *J. Mater. Chem. A* **2020**, *8*, 15042–15050.
- [44] a) Z. Liu, G. Z. Li, T. Cui, A. Borodin, C. Kuhl, F. Endres, *J. Solid State Electrochem.* **2018**, *22*, 91–101; b) X. S. Zhang, Z. X. Pei, C. J. Wang, Z. W. Yuan, L. Wei, Y. Q. Pan, A. Mahmood, Q. Shao, Y. Chen, *Small* **2019**, *15*, 1903817.
- [45] L. Han, H. L. Huang, X. B. Fu, J. F. Li, Z. L. Yang, X. J. Liu, L. K. Pan, M. Xu, *Chem. Eng. J.* **2020**, *392*, 123733.
- [46] L. Y. Yang, L. Song, Y. Feng, M. J. Cao, P. C. Zhang, X. F. Zhang, J. F. Yao, *J. Mater. Chem. A* **2020**, *8*, 12314–12318.
- [47] D. W. Wang, Z. M. Pan, Z. M. Lu, *Microporous Mesoporous Mater.* **2020**, *306*, 110445.
- [48] N. S. Arul, L. S. Cavalcante, J. I. Han, *J. Solid State Electrochem.* **2018**, *22*, 303–313.
- [49] H. T. Sun, J. Zhu, D. Baumann, L. L. Peng, Y. X. Xu, I. Shakir, Y. Huang, X. F. Duan, *Nat. Rev. Mater.* **2019**, *4*, 45–60.
- [50] J. Qian, X. Wang, L. Chai, L.-F. Liang, T.-T. Li, Y. Hu, S. Huang, *Cryst. Growth Des.* **2018**, *18*, 2358–2364.
- [51] N. N. Chang, T. Y. Li, R. Li, S. N. Wang, Y. B. Yin, H. M. Zhang, X. F. Li, *Energy Environ. Sci.* **2020**, *13*, 3527–3535.
- [52] a) H. D. Yoo, I. Shterenberg, Y. Gofer, G. Gershinsky, N. Pour, D. Aurbach, *Energy Environ. Sci.* **2013**, *6*, 2265–2279; b) D. Aurbach, Y. Cohen, M. Moshkovich, *Electrochem. Solid-State Lett.* **2001**, *4*, A113–A116; c) C. Ling, D. Banerjee, M. Matsui, *Electrochim. Acta* **2012**, *76*, 270–274; d) M. M. Huie, D. C. Bock, E. S. Takeuchi, A. C. Marschilok, K. J. Takeuchi, *Coord. Chem. Rev.* **2015**, *287*, 15–27.
- [53] H. D. Yoo, I. Shterenberg, Y. Gofer, R. E. Doe, C. C. Fischer, G. Ceder, D. Aurbach, *J. Electrochem. Soc.* **2014**, *161*, A410–A415.
- [54] a) L. Luo, K. Q. Zhou, R. Q. Lian, Y. Z. Lu, Y. C. Zhen, J. S. Wang, S. Mathur, Z. S. Hong, *Nano Energy* **2020**, *77*, 104716; b) L. Luo, Y. C. Zhen, Y. Z. Lu, K. Q. Zhou, J. X. Huang, Z. G. Huang, S. Mathur, Z. S. Hong, *Nanoscale* **2020**, *12*, 230–238.
- [55] T. Lu, Z. H. Zhang, B. B. Chen, S. M. Dong, C. D. Wang, A. B. Du, L. L. Wang, J. Ma, G. L. Cui, *Mater. Today* **2020**, *17*, 100450.
- [56] a) T. Y. Liu, Z. P. Zhou, Y. C. Guo, D. Guo, G. L. Liu, *Nat. Commun.* **2019**, *10*, 675; b) Z. H. Huang, Y. Song, D. Y. Feng, Z. Sun, X. Q. Sun, X. X. Liu, *ACS Nano* **2018**, *12*, 3557–3567; c) Q. Z. Zhang, D. Zhang, Z. C. Miao, X. L. Zhang, S. L. Chou, *Small* **2018**, *14*.
- [57] P. Meister, V. Kuepers, M. Kolek, J. Kasnatscheew, S. Pohlmann, M. Winter, T. Placke, *Batteries Supercaps* **2021**, *4*, 504.
- [58] J. Z. Niu, Z. H. Zhang, D. Aurbach, *Adv. Energy Mater.* **2020**, *10*, 2000697.
- [59] X. W. Miao, J. Yang, W. J. Pan, H. C. Yuan, Y. N. Nuli, S. Hirano, *Electrochim. Acta* **2016**, *210*, 704–711.
- [60] J. H. Lang, C. L. Jiang, Y. Fang, L. Shi, S. J. Miao, Y. B. Tang, *Adv. Energy Mater.* **2019**, *9*, 1901099.
- [61] a) A. Ponrouch, C. Frontera, F. Barde, M. R. Palacin, *Nat. Mater.* **2016**, *15*, 169; b) S. Ghaytani, Y. L. Liang, F. L. Wu, Y. Jing, H. Dong, K. K. Rao, X. W. Chi, F. Fang, Y. Yao, *Adv. Sci.* **2017**, *4*, 1700465.
- [62] D. He, Y. Gao, Y. C. Yao, L. Wu, J. Zhang, Z. H. Huang, M. X. Wang, *Front. Chem.* **2020**, *8*, 719.
- [63] L. Y. Liu, Y. C. Wu, P. Rozier, P. L. Taberna, P. Simon, *Research* **2019**, *2019*, UNSP 6585686.
- [64] A. L. Lipson, S. Kim, B. F. Pan, C. Liao, T. T. Fister, B. J. Ingram, *J. Power Sources* **2017**, *369*, 133–137.
- [65] N. Emery, C. Herold, P. Lagrange, *J. Solid State Chem.* **2005**, *178*, 2947–2952.
- [66] J. Park, Z. L. Xu, G. Yoon, S. K. Park, J. Wang, H. Hyun, H. Park, J. Lim, Y. J. Ko, Y. S. Yun, K. Kang, *Adv. Mater.* **2020**, *32*, 1904411.
- [67] M. Greaves, S. Barg, M. A. Bissett, *Batteries & Supercaps* **2020**, *3*, 214–235.
- [68] Y. L. Jie, Y. S. Tan, L. M. Li, Y. H. Han, S. T. Xu, Z. C. Zhao, R. G. Cao, X. D. Ren, F. Y. Huang, Z. W. Lei, G. H. Tao, G. Q. Zhang, S. H. Jiao, *Angew. Chem. Int. Ed.* **2020**, *59*, 12689–12693.
- [69] J. J. Qian, X. Wang, L. L. Chai, L. F. Liang, T. T. Li, Y. Hu, S. M. Huang, *Cryst. Growth Des.* **2018**, *18*, 2358–2364.
- [70] S. Cho, J. Han, J. Kim, Y. Jo, H. Woo, S. Lee, A. A. Ahmed, H. C. Chavan, S. M. Pawar, J. L. Gunjakar, J. Kwak, Y. Park, A. I. Inamdar, H. Kim, H. Kim, H. Im, *Curr. Appl. Phys.* **2017**, *17*, 1189–1193.
- [71] Q. F. Li, N. J. Bjerrum, *J. Power Sources* **2002**, *110*, 1–10.
- [72] F. X. Wang, Z. C. Liu, X. W. Wang, X. H. Yuan, X. W. Wu, Y. S. Zhu, L. J. Fu, Y. P. Wu, *J. Mater. Chem. A* **2016**, *4*, 5115–5123.
- [73] M. C. Lin, M. Gong, B. G. Lu, Y. P. Wu, D. Y. Wang, M. Y. Guan, M. Angell, C. X. Chen, J. Yang, B. J. Hwang, H. J. Dai, *Nature* **2015**, *520*, 325.
- [74] J. Xu, P. Jiang, X. L. Liang, R. J. Tian, Y. M. Liu, *Fullerenes Nanotubes Carbon Nanostruct.* **2020**, *29*, 21–27.
- [75] Z. Li, K. Xiang, W. T. Xing, W. C. Carter, Y. M. Chiang, *Adv. Energy Mater.* **2015**, *5*, 1401410.
- [76] D. J. Kim, D. J. Yoo, M. T. Otley, A. Prokofjevs, C. Pezzato, M. Owczarek, S. J. Lee, J. W. Choi, J. F. Stoddart, *Nat. Energy* **2019**, *4*, 51–59.
- [77] S. Liu, J. J. Hu, N. F. Yan, G. L. Pan, G. R. Li, X. P. Gao, *Energy Environ. Sci.* **2012**, *5*, 9743–9746.
- [78] L. X. Geng, G. C. Lv, X. B. Xing, J. C. Guo, *Chem. Mater.* **2015**, *27*, 4926–4929.
- [79] B. Tan, S. H. Han, W. B. Luo, Z. S. Chao, J. C. Fan, M. Y. Wang, *J. Alloys Compd.* **2020**, *842*, 156110.
- [80] Z. C. Zhao, Z. Q. Hu, Q. Li, H. S. Li, X. Zhang, Y. D. Zhuang, F. Wang, G. H. Yu, *Nano Today* **2020**, *32*, 100870.
- [81] H. Y. Xu, T. W. Bai, H. Chen, F. Guo, J. B. Xi, T. Q. Huang, S. Y. Cai, X. Y. Chu, J. Ling, W. W. Gao, Z. Xu, C. Gao, *Energy Storage Mater.* **2019**, *17*, 38–45.
- [82] Z. J. Yu, S. Q. Jiao, S. Li, X. D. Chen, W. L. Song, T. Teng, J. G. Tu, H. S. Chen, G. H. Zhang, D. N. Fang, *Adv. Funct. Mater.* **2019**, *29*, 1806799.
- [83] L. Balo, Shalu, H. Gupta, V. K. Singh, R. K. Singh, *Electrochim. Acta* **2017**, *230*, 123–131.
- [84] Y. H. Feng, S. H. Chen, J. Wang, B. A. Lu, *J. Energy Chem.* **2020**, *43*, 129–138.

Manuscript received: December 8, 2020

Revised manuscript received: February 6, 2021

Accepted manuscript online: February 10, 2021

Version of record online: March 4, 2021